Genome-wide association study identifies novel susceptibility loci for *KIT* D816V positive mastocytosis

Gabriella Galatà[1], Andrés C. García-Montero[2,3], Thomas Kristensen[4,5], Ahmed A.Z. Dawoud[1], Javier I. Muñoz-González[2,3], Manja Meggendorfer[6], Paola Guglielmelli[7], Yvette Hoade[1], Ivan Alvarez-Twose[8], Christian Gieger[9,10,11,12], Konstantin Strauch[9,13,14], Luigi Ferrucci[15], Toshiko Tanaka[15], Stefania Bandinelli[16], Theresia M. Schnurr[17], Torsten Haferlach[6], Sigurd Broesby-Olsen[5,18,19], Hanne Vestergaard[5,20], Michael Boe Møller[4,5], Carsten Bindslev-Jensen[5,18,19], Alessandro M Vannucchi[7], Alberto Orfao[2,3], Deepti Radia[21], Andreas Reiter[22], Andrew J. Chase[1,23], Nicholas C.P. Cross [1,23*] and William J. Tapper[1*]

[1]Faculty of Medicine, University of Southampton, Southampton, UK
[2]Institute of Biomedical Research of Salamanca (IBSAL), Salamanca, Spain
[3]Servicio de Citometría, Departamento de Medicina, CIBERONC, and Instituto de Biología Molecular y Celular del Cáncer, CSIC/Universidad de Salamanca, Salamanca, Spain
[4]Department of Pathology, Odense University Hospital, Odense, Denmark
[5]Mastocytosis Centre Odense University Hospital (MastOUH), Odense, Denmark
[6]MLL Munich Leukemia Laboratory, Munich, Germany
[7]Centro di Ricerca e Innovazione per le Malattie Mieloproliferative, Azienda Ospedaliera Universitaria Careggi, Dipartimento di Medicina Sperimentale e Clinica, Università Degli Studi di Firenze, Firenze, Italy
[8]Instituto de Mastocitosis de Castilla La Mancha, Hospital Virgen del Valle, Toledo, Spain
[9]Institute of Genetic Epidemiology, Helmholtz Zentrum München – German Research Center for Environmental Health (GmbH), Neuherberg, Germany
[10]German Centre for Cardiovascular Research (DZHK) Partner Site Munich Heart Alliance, Munich, Germany
[11]Research Unit of Molecular Epidemiology, Helmholtz Zentrum München, German Research Center for Environmental Health, Neuherberg, Germany
[12]German Center for Diabetes Research (DZD), Neuherberg, Germany
[13]Chair of Genetic Epidemiology, IBE, Faculty of Medicine, LMU Munich, Munich, Germany
[14]Institute of Medical Biostatistics, Epidemiology and Informatics (IMBEI), University Medical Center, Johannes Gutenberg University, Mainz, Germany
[15]Longitudinal study section, Translation Gerontology Branch, National Institute on Aging, Baltimore, MD 21224, USA
[16]Geriatric Unit, Azienda USL Toscana centro, Firenze, Florence, Italy
[17]Novo Nordisk Foundation Center for Basic Metabolic Research, Faculty of Health and Medical Sciences, University of Copenhagen, Copenhagen, Denmark
[18]Department of Dermatology and Allergy Centre, Odense University Hospital, Odense, Denmark
[19]Odense Research Center for Anaphylaxis (ORCA), Odense University Hospital, Odense, Denmark
[20]Department of Hematology, Odense University Hospital, Odense, Denmark
[21]Department of Clinical Haematology, Guys and St Thomas' NHS Hospitals, London, UK
[22]University Hospital Mannheim, Heidelberg University, Mannheim, Germany
[23]Wessex Regional Genetics Laboratory, Salisbury NHS Foundation Trust, Salisbury, UK

*These authors contributed equally to this work

Correspondence to:

Professor N.C.P. Cross
Wessex Regional Genetics Laboratory
Salisbury NHS Foundation Trust
Salisbury SP2 8BJ, UK

Tel: +(44) 1722 429080
Fax: +(44) 1722 331531
email: ncpc@soton.ac.uk

Abstract

Mastocytosis is a rare myeloid neoplasm characterised by uncontrolled expansion of mast cells, driven in >80% of cases by acquisition of the *KIT* D816V mutation. To explore the hypothesis that inherited variation predisposes to mastocytosis, we performed a two stage genome-wide association study, analysing 1,035 patients with *KIT* D816V positive disease and 17,960 healthy controls from five European populations. After quality control, we tested 592,007 SNPs at stage-1 and 75 SNPs at stage-2 for association using logistic regression and performed a fixed effects meta-analysis to combine evidence across the two stages. From the meta-analysis, we identified three intergenic SNPs associated with mastocytosis that achieved genome-wide significance without heterogeneity between cohorts, rs4616402 (P_{meta}=1.37x10^{-15}, OR=1.52), rs4662380 (P_{meta}=2.11x10^{-12}, OR=1.46) and rs13077541 (P_{meta}=2.10x10^{-9}, OR=1.33). Expression quantitative trait analyses demonstrated that rs4616402 is associated with the expression of *CEBPA* (P_{eQTL}=2.3x10^{-14}), a gene encoding a transcription factor known to play a critical role in myelopoiesis. The role of the other two SNPs is less clear: rs4662380 is associated with expression of the long non-coding RNA gene *TEX41* (P_{eQTL}=2.55x10^{-11}) whereas rs13077541 is associated with the expression of *TBL1XR1,* which encodes transducin (β)-like 1 X-linked receptor 1 (P_{eQTL}=5.70x10^{-8}). In cases with available data and non-advanced disease, rs4616402 was associated with age at presentation (P=0.009; beta=4.41; n=422). Additional focused analysis identified suggestive associations between mastocytosis and genetic variation at *TERT*, *TPSAB1/TPSB2* and *IL13*. These findings demonstrate that multiple germline variants predispose to *KIT* D816V positive mastocytosis and provide novel avenues for functional investigation.

Introduction

Mastocytosis (MIM: 154800) is an uncommon myeloid neoplasm characterized by expansion and accumulation of clonal mast cells in one or more organ systems, including bone marrow, skin, liver, spleen, and gastrointestinal tract. The extent of organ infiltration and organ damage serve as the basis for classification as cutaneous mastocytosis (CM) or systemic mastocytosis (SM)[1]. CM is typically found in children, whilst most adults with mastocytosis have SM with involvement of the bone marrow. Six main subtypes of SM are recognised: indolent SM (ISM) and smouldering systemic mastocytosis (SMM) are relatively benign forms that usually have a stable clinical course over many years. In contrast, SM with an associated hematologic neoplasm (SM-AHN), aggressive SM (ASM) and mast cell leukemia (MCL), collectively known as advanced SM (advSM), are associated with a poor prognosis[2]. ISM is the most common of the 6 subtypes, accounting for 80% of SM cases[3].

Approximately 80-90% of adult SM cases across all subtypes test positive for the somatic mutation, *KIT* c.2447A>T; p.(Asp816Val), usually referred to as *KIT* D816V. Due to the nature of the disease, the mutant allele frequency is often very low, particularly in peripheral blood samples, and sensitive methods are needed for its detection[4]. *KIT* D816V mutation burden, serum tryptase and β2-microglobulin levels correlate with disease burden and severity[5-8], and for advSM additional somatic mutations in *SRSF2*, *ASXL1* and *RUNX1* indicate an adverse prognosis[9-11].

Mastocytosis is usually a sporadic disorder but familial forms have been described, often in association with inherited, weakly activating *KIT* mutations[12; 13]. Very occasionally, familial clustering of *KIT* D816V has been observed but in all cases this mutation is somatically acquired[14] and, as a strongly activating variant, *KIT* D816V is believed to be incompatible with normal embryonic development and thus not transmissible through the germline. Other lines of evidence suggest the possibility of a broader role for genetic variation in mastocytosis. The presence of germline variants in genes known to be somatically mutated in myeloid disorders were one of several factors related to adverse clinical outcome in SM[11]. Studies of Mast Cell Activation Disease (MCAD), a disorder that overlaps with SM, indicate a substantial excess of symptoms in first-degree relatives of affected individuals which might suggest a common genetic susceptibility[15; 16]. Several constitutional genetic variants have been associated with the development of different mastocytosis phenotypes in relatively small candidate gene studies[17-21], and a recent single stage genome wide association study (GWAS) of 234 cases[22]. Finally, it has been clearly established that constitutional genetic variation at several loci predispose to other myeloproliferative neoplasms (MPN)[23; 24].

To determine whether common genetic variation plays a role in predisposition to mastocytosis, we have performed a robust two stage GWAS focusing on cases that tested positive for *KIT* D816V

regardless of clinical subtype to help to ensure a genetically homogeneous cohort. We anticipate that the identification of validated genetic markers associated with mastocytosis will provide novel lines of investigation to understand this complex disorder.

Methods

Discovery and replication cohorts

Prior to quality control (QC), the stage 1 discovery cases consisted of 479 *KIT* D816V positive mastocytosis patients recruited from the UK (n=329) and Germany (n=150). These cases were compared with healthy controls from the UK Wellcome Trust Case Control Consortium (WTCCC2, n=5,200)[25] and the German Cooperative Health Research in the Region of Augsburg study (KORA, n=4,397), respectively[26]. At stage-2, 666 independent *KIT* D816V positive replication cases were recruited from Spain (n=399), Denmark (n=185) and Italy (n=82) and compared to published population controls from the Spanish National DNA Bank (SNDNAB, n=1,062)[27; 28], a Danish study of ischaemic heart disease (Inter99, n=6,184)[29; 30] and the Italian Invecchiare in Chianti study (InCHIANTI, n=1,210)[31; 32]. Participants provided informed consent for sampling according to the Declaration of Helsinki. The number of samples that were recruited and used for analysis after QC in the discovery and replication stages is shown in Table S1. An overview of the two stage study design and sample numbers is shown in Figure S1. All mastocytosis cases were adults diagnosed using standard procedures. Further details on the 5 cohorts are provided in the Supplementary Methods.[2; 4]

Genotyping

DNA was extracted from peripheral blood or bone marrow. The stage-1 cases were genotyped for 960,919 SNPs using Infinium OmniExpress exome chips (version 8_1.4_A1) and the Genome Studio software (GSGT Version 1.9.4) at the Clinical Research Facility in Edinburgh. These data are available on request from ArrayExpress (accession number E-MTAB-9358). The stage-2 cases were genotyped for 92 SNPs using custom designed Kompetitive Allele Specific PCR (KASP) at LGC[33]. Genotypic data for the control cohorts were obtained from published studies. In WTCCC2, genotypes were called separately in the NBS and BBC cohorts using Illumina 1.2M Duo chips and the Illumina's programme to call SNPs with a posterior probability >0.95[34]. KORA controls were genotyped for 2,443,177 SNPs using the Illumina human Omni chip (version 2.5-4v1_B) in KORA_A (a subset of follow-up F3 of the population based survey KORA S3) and 730,372 SNPs using Illumina human Omni express chips (version 12v1_H) in KORA_B (an independent subset of KORA S3/F3). Controls from SNDNAB, Inter99 and InCHIANTI were genotyped using Illumina Global Screening arrays, Illumina HumanOmniExpress-

24 (versions 1.0A and 1.1A) and Illumina Infinium HumanHap 550K SNP arrays which include 18, 90 and 45 of the SNPs selected for replication respectively. Genotypes for the remaining SNPs were determined by imputation.

Quality control

Standard GWAS QC measures[35] were applied to the genotypic data prior to analysis using Plink[36]. These measures included genotype missingness (per sample and per SNP), minor allele frequency (MAF), Hardy Weinberg equilibrium (HWE), heterozygosity (Figure S2), sex inference, cryptic relatedness, strand orientation and population stratification using multidimensional scaling (MDS) (Figure S3). Since the cases and controls were genotyped separately, SNPs were excluded if they had modest deviation from Hardy-Weinberg equilibrium (HWE) in controls (P-value <0.001) or extreme deviation in cases (P-value $\leq 1x10^{-10}$) which most likely reflects poor genotyping rather than disease association[37]. The number of SNPs and samples removed by these QC measures is shown in Table S1. QC and imputation of the stage 2 controls has previously been described.[28-32] Full details regarding the QC and imputation procedures are given in the Supplementary methods.

Imputation

Imputation of the discovery cohorts was used to increase SNP density and enable fine mapping around significant loci. SNPs were imputed using the Sanger imputation server[38] which used EAGLE2 for pre-phasing into the Haplotype Reference Consortium (HRC release 1.1), and positional Burrows-Wheeler transform (PBWT) for imputation. Imputed genotypes were quality controlled by excluding SNPs with info score <0.80, posterior genotype probabilities less than 0.99, minor allele frequency less than 1%, greater than 10% missing genotypes or extreme deviation from HWE (P-value $\leq 1x10^{-10}$).

Statistical analysis

SNPs were tested for association using binary logistic regression in Plink. A fixed effects inverse variance-weighted meta-analysis was carried out using Plink to combine evidence from the stage-1 cohorts (UK and Germany) and to determine the final effect sizes and significance levels by combining evidence across stages-1 and 2. Heterogeneity between studies was estimated using the χ^2-based Cochran's Q statistic and the I^2 statistic which describes the percentage of variation across studies that is due to heterogeneity rather than chance. To examine the effectiveness of the QC measures and assess evidence for any systematic biases the qqnorm and qqplot procedures in R were used to construct quantile-quantile (QQ) plots for the stage-1 analysis of the UK and German cohorts and the stage-1 meta-analysis (Figure S4). Samples with evidence of non-Caucasian ancestry were excluded rather than adjusting the association analysis for population stratification. To examine the effect of

this decision, the ancestry outliers were retained and the stage 1 analyses were repeated with adjustment for the first two principal components from the MDS analysis (Figure S5 and Table S2).

The results from the stage-1 meta-analysis were visualised and interpreted using the qqman package[39] in R to create a Manhattan plot (Figure 1) and the FUMA software to generate regional plots[40]. Results from the final meta-analysis of stages 1 and 2 were displayed in a forest plot using Stata (Figure 2).

The power to detect SNPs associated with SM was estimated using the genetic power calculator[41] under a multiplicative genetic risk model and a type 1 error rate of $5x10^{-8}$ (Figure S6). A range of genotype relative risks (1.1-2.0) and risk allele frequencies (MAF 0.05-0.4) were used to estimate power assuming a disease prevalence of 1 in 100,000[42] and unselected controls.

Selection of SNPs for replication

To minimize false positives and the potential for overlooking signals with compelling functional evidence but modest significance, the following method was used to select SNPs for follow-up at stage-2. First a clumping procedure in Plink was used to generate a shortlist of index SNPs ($P<0.001$) with support from correlated SNPs (SNPs $r2>0.5$, within 500 kb and $P<0.01$) based on the stage 1 meta-analysis. From this shortlist, 92 index SNPs were selected for replication with priority, but not exclusivity, given to SNPs that were either located in or flanked by a gene with functional relevance according to annotation from GeneAlacart[43]. Relevant functions were signal transduction components, hematopoiesis, myeloid leukemia, myeloproliferative or mast cell conditions from GeneAlacart[43]. A total of 44 SNPs were selected with functional relevance. The number of selected SNPs was then infilled to 82 by selecting the most significant remaining index SNPs. An additional 10 SNPs were selected as backups and to add support to the most promising signals in terms of either their biological relevance, individual significance or level of support from correlated SNPs.

Identification of chromosomal abnormalities

Regions of acquired uniparental disomy (aUPD) and copy number gains or losses were identified in the stage 1 SM patients using B allele frequency (BAF) segmentation[44] followed by post processing to select likely somatic events as described[45] and manual review of all BAF plots (Figure S7). See supplementary methods for further details.

Functional annotation of variants

The biological relevance of regions containing genome-wide significant SNPs was explored using HaploReg (version 4.1)[46] to annotate the lead SNP and their proxies ($r^2 \geq 0.8$) with respect to histone modification, sequence conservation using genomic evolutionary rate profiling (GERP)[47], estimated

pathogenicity using combined annotation-dependent depletion scores (CADD)[48], predicted effect on protein binding using RegulomeDB[49] scores (SNPs scoring ≤3 are likely to affect binding) and previous associations with clinical phenotypes using the NHGRI-EBI GWAS catalog[50]. Additionally, candidate regions were annotated against a 15 state chromatin model[51] in primary hematopoietic stem cells (E035) and a myeloid leukemia cell line (K562). This model categorizes non coding DNA into active or repressed states that are respectively enriched and depleted for phenotype-associated SNPs[52]. To gain further functional insight, expression and methylation quantitative trait loci analyses (eQTL and mQTL) were performed on the lead SNP and their proxies (r^2 ≥0.8) using GTEx v8[53] and QTLbase[54]. Finally, LNCipedia[55] and the Cancer LncRNA Census (CLC)[56] were used to investigate the function of long non-coding RNA (lncRNA).

Association with clinical features

Diagnostic and phenotypic variables for initial diagnosis (advanced = ASM, SM-AHN, MCL; non-advanced = all other subtypes), the presence or absence of skin lesions (yes or no), gender, baseline serum tryptase (ng/mL) and age were available for most of the Spanish (n=369) and Italian (n=81) patients, but not other cohorts. Three categorical variables (initial diagnosis, skin lesions and sex) were tested for association with allelic counts for the 3 significant SNPs using Fisher's exact test. Continuous variables (tryptase and age) were tested using linear regression following Kolmogorov-Smirnov checks for normal distribution and normalisation of tryptase levels using quantile transformation. A fixed-effect inverse variance-weighted meta-analysis was used to combine evidence from the two cohorts.

Results

Discovery stage

After quality control of the stage 1 data, 592,007 SNPs were tested for association with *KIT* D816V positive mastocytosis using binary logistic regression in the UK (274 cases versus 5176 controls) and German cohorts (140 cases versus 4328 controls) (Table S1). Summary statistics from these analyses were combined using a fixed effects meta-analysis which are available from LocusZoom[57]. The quantile-quantile (QQ) plots for each analysis and their low genomic inflation factors (λ ≤1.038) demonstrate a close agreement with the null hypothesis until the tail of the distribution where SNPs with *P*-values less than 10^{-4} become more significant than expected by chance alone (Figure S4). Consequently, systematic biases such as the separate genotyping of our cases and controls, residual population stratification or clonal somatic changes are unlikely to account for the significance of these

SNPs. A Manhattan plot summarising the results of the stage 1 meta-analysis is shown in Figure 1. A total of 18 SNPs were identified with suggestive *P*-values ($P \leq 1x10^{-5}$).

Replication and final meta-analysis

According to the number of samples that passed QC and using a multiplicative disease model, the stage 1 analysis was estimated to have 80% power to detect common SNPs (MAF=0.4) with a relative risk (RR) of 1.56, and rare SNPs (MAF=0.1) with a RR of 1.82 (Figure S6a). Due to the potential to overlook SNPs with smaller effect sizes, we used a set of selection criteria rather than significance alone (see Methods) to identify 92 SNPs for replication. These SNPs were selected to have support from correlated SNPs and were either; the most significant (n=38), or surpassed a moderate significance threshold (P<0.001) and were located in or flanked by a functionally relevant gene (n=44), or were selected as backups for the most promising signals (n=10). One SNP achieved genome-wide significance in the stage 1 analysis, rs7884433, but it was not selected for replication because it lacked support from any of the SNPs in strong LD and is thus likely to be a technical artefact.

Of the 92 SNPs selected, 75 were successfully genotyped in 666 *KIT* D816V mastocytosis cases from Spain, Denmark and Italy. Additional controls (n=8,456) from the same populations that had previously been genotyped were used for comparison. After QC, 621 cases and all the controls remained for analysis. All SNPs passed QC in cases although 19 were excluded from the Spanish controls due to per SNP missingness (≥10%) following imputation. Samples were tested for association with SM as three separate cohorts using binary logistic regression. The final significance levels and effect sizes were determined using a fixed effects inverse variance-weighted meta-analysis to combine evidence from stages 1 and 2. This meta-analysis identified three intergenic SNPs with genome-wide significance, rs4616402 ($P_{meta}=1.37x10^{-15}$), rs4662380 ($P_{meta}=2.11x10^{-12}$) and rs13077541 ($P_{meta}=2.10x10^{-9}$) (Table 1). Results for the three SNPs reaching genome-wide significance are summarised in a forest plot which shows that each SNP is significant in four of the five cohorts tested and that there is evidence for the same trend in the remaining population (Figure 2). Cochran's Q test and I^2 statistics showed that for each SNP there was no evidence of heterogeneity between cohorts. Results from the meta-analysis of stages-1 and 2 for all SNPs tested are shown in Table S3.

To investigate the possibility of residual population stratification, the stage 1 analyses were repeated without removing 26 samples with evidence of outlying ancestry (Table S1) and adjusting the association analysis using the first two principal components from MDS. The top three SNPs retained genome-wide significance, with rs4662380 and rs13077541 becoming slightly more significant (Table S2), which suggests an absence of residual population stratification in the original analysis.

Functional annotation and candidate gene mapping

To explore the functional relevance of the regions associated with mastocytosis, we used HaploReg and RegulomeDB to determine if the risk SNP or their proxies (r^2 ≥0.8) were located in regions with potential regulatory functions based on chromatin modification, DNA methylation and alteration of transcription factor (TF) binding motifs (Table S4). To gain further functional insight, we performed expression and methylation quantitative trait loci analyses (eQTL and mQTL) on the lead SNP and their proxies using GTEx v8[53] and QTLbase[54]. Finally, the stage-1 meta-analysis was repeated using imputation to enable fine mapping around the lead SNPs and to generate association results for proxies which had not been directly genotyped.

The most significant SNP, rs4616402, confers a 1.52 fold increased risk of developing mastocytosis and is situated in an intergenic region on chromosome 19 between a solute carrier gene (*SLC7A10*, 36.8Kb downstream) and a gene encoding a transcription factor (*CEBPA*, 37.2kb downstream) that coordinates proliferation and differentiation of myeloid progenitor cells (Figure 3a). Using QTLbase we found that rs4616402 is strongly associated with the expression of *CEBPA* in whole blood according to data from three previous eQTL studies (P_{eQTL}=2.30x10^{-14}; P_{eQTL}= 2.96x10^{-11}; P_{eQTL}= 9.20x10^{-9})[58-60]. There is no evidence that *SLC7A10* has a role in carcinogenesis, including myeloid malignancies, and no additional SNPs were identified in strong LD with rs4616402. However, there is weak evidence that rs4616402 may have functional consequences according to the RegulomeDB score (score=4). The chromatin surrounding rs4616402 is characterised as an enhancer (7_Enh) in primary hematopoietic stem cells due to an enrichment of the H3K4me1 signature. Additionally, the risk allele is predicted to alter three TF binding motifs (Arnt_1, Gm397 and Hmx_1, Table S4).

The second most significant SNP, rs4662380, increases the risk of developing mastocytosis by 1.46 fold and is located in the first intron of a lincRNA gene (*LINC01412*) (Figure 3b). Twelve additional SNPs in the *LINC01412* gene were identified in strong LD with the lead. Three of these proxies are located in chromatin enhancers (7_Enh: rs6722387, rs16823865, rs13413446) in primary hematopoietic stem cells and one is located in a flanking active transcription start site (2_TssAFlnk: rs16823855) in K562 (Table S4). The RegulomeDB scores indicate that two of the proxies are likely to affect TF binding, rs4662227 (score=2c) and rs13413446 (score=3a) while the remaining SNPs are estimated to have weak evidence for functional consequences. However, using the GWAS catalog[50] we found that one of the remaining proxies, rs16823866, was strongly associated with white blood cell counts in two previous studies (P=4x10^{-18} and P=6x10^{-11})[61; 62]. Finally, using QTLbase we found that the lead SNP (P_{eQTL}=2.55x10^{-11}) and four proxies including rs16823866 (P_{eQTL}=2.55x10^{-11}) were strongly associated with the expression of the nearby gene *TEX41* in neutrophils[63].

The final SNP, rs13077541, is associated with a 1.33 fold increase in risk of developing mastocytosis and is located in an intergenic region of chromosome 3 between transducin beta like 1 X-linked receptor 1 (*TBL1XR1*, 10.6kb upstream) and another lincRNA RNA gene (*LINC00501*, 86.5kb upstream) (Figure 3c). Fifty three additional SNPs were identified in strong LD with the lead including twenty seven intronic SNPs in *TBL1XR1* (Table S4). Eleven of these proxies are located in active chromatin regions including three in an active transcription start site (1_TssA: rs12493005, rs12486557, rs34302523) and two in a 5' transcribed region (3_TxFlnk: rs35072945, rs34311793) in K562. The RegulomeDB scores indicate that five of the proxies are likely to affect binding (score2a-c: rs6790639, rs34302523, rs6772872, rs7616138 and rs1920131). Of these, rs6790639 is particularly relevant as the PU.1 TF, which is encoded by the Spi-1 proto-oncogene (*SPI1*), has been shown to bind to this region inK562 using ChIP sequencing[64]. PU.1, together with other TFs, regulates the expression of genes involved myelopoiesis[65]. Using QTLbase we found that the lead SNP (P_{eQTL}=5.70x10^{-8}) and one of the proxies, rs16823866 (P_{eQTL}=9.52x10^{-9}), were strongly associated with the expression of *TBL1XR1* in CD4+ naïve T cells[63].

Association with clinical features

To determine if variants that predispose to the development of mastocytosis relate to particular clinical features, we used Fisher's exact tests and linear regression to correlate allelic counts for the three significant SNPs with clinical phenotypes in the Spanish and Italian cohorts (Table 2), the only cases for which clinical information was available. A significant association was identified between rs4616402 and age at presentation (n=422; P=0.009; beta=4.41) in patients with non-advanced disease that remained significant after correction for multiple testing. No association with age was seen in the much smaller group of cases (n=26) with advanced disease, a subgroup for which additional mutations may be a confounding factor. In cases, the age of onset was estimated to increase by 4.41 years per risk allele. No associations were seen with baseline tryptase levels, gender, skin lesions or disease phenotype.

Association with *TPSAB1* and *TPSB2*

Increased copy number variation at *TPSAB1*, the gene at 16p13 encoding α-tryptase, is associated with elevated serum tryptase levels in hereditary α-tryptasemia[66]. Our analysis did not include direct copy number analysis of this gene, however a recent study linked *TPSAB1* duplications with three SNPs including rs58124832[67]. This SNP was genotyped at stage 1 and met our criteria for analysis at stage

2, yielding a suggestive overall association with SM (P_{meta}=9.03x10^{-6}). The Cochran's Q test and I^2 statistics showed no evidence of heterogeneity between cohorts, however the association was significant in only three cohorts (P_{German}=0.0058, P_{UK}=0.0042, $P_{Spanish}$=0.05). The eQTL analysis showed that rs58124832 is strongly associated with the expression of *TPSAB1* (P_{eQTL}<1.9x10^{-58}) and *TPSB2* (tryptase-β2; P_{eQTL}=1.96x10^{-75}) in blood.

Association with *TERT*

Several *TERT* SNPs have been identified as risk factors for the development of hematological malignancies, including MPN, as well as some solid tumours. Our stage 1 analysis included rs2853677, which has been linked to both MPN and *JAK2* V617F associated clonal hematopoiesis[24]. This SNP marginally failed to meet our criteria for analysis at stage 2, however the stage 1 meta-analysis for directly genotyped UK and German cases showed P_{meta}=0.0011, suggesting the possibility of an association. To examine this in more detail we imputed genotypes for 64 additional SNPs spanning *TERT* and tested their association with SM. As shown in Table S5, 7 SNPs achieved P values of <0.001. The strongest of these was for rs7726159 (P_{meta}=8x10^{-5}), an established risk SNP for multiple cancer types[68]. We identified one secondary association at *TERT* for rs2853677 which remained significant after conditioning on rs7726159 ($P_{conditional}$= 0.035). No associations were seen with other SNPs that predispose to MPN[69] or clonal hematopoiesis of indeterminate potential[70] in our stage 1 data (Table S6).

Associations with other genetic factors

To the best of our knowledge, 14 SNPs have been associated with the development or phenotype of human mastocytosis in published studies[17-22]. Of these, 11 were directly genotyped or could be imputed from our stage 1 data (Table S7) but only one of these was significant: rs1800925 in the promoter region of *IL13* at 5q31 ($P_{imputed}$=0.008). This SNP has been linked to the development of adult SM and serum interleukin-13 levels[18] and inflammatory disorders such as chronic obstructive pulmonary disease[71].

Discussion

Despite being characterised by a common somatic oncogenic driver mutation, mastocytosis is a complex disorder with a broad range of clinical phenotypes and outcomes. In this study we have identified constitutional genotype as an additional factor contributing to the heterogeneity of

mastocytosis. The use of a molecular definition for cases rather than clinically-defined subtypes and careful ethnicity matching of cases and controls aimed to reduce the chance of heterogeneity both in the primary and replication cohorts. Thus, with a relatively modest cohort size for a GWAS, we were able to identify and validate 3 novel SNPs that achieved genome wide significance, and additional suggestive associations at *TERT*, *TPSAB1/TPSB2* and *IL13* that merit further investigation. Notably, apart from rs1800925 (*IL13*), we did not confirm any of the previously published associations derived from candidate gene studies and a recent GWAS that did not include a replication cohort (Table S6). In addition, we found no evidence that genetic variation at *KIT* is associated with acquisition of *KIT* D816V, unlike the finding in MPN that *JAK2* haplotype strongly influences the probability of acquiring *JAK2* V617F[72].

Theoretically, common genetic variation may influence mastocytosis by distinct mechanisms, for example by promoting or favouring the outgrowth of a *KIT* D816V positive clone that arose by random mutation (fertile ground hypothesis); by increasing the probability that a *KIT* D816V mutation arises in a stem cell (hypermutability hypothesis); or by promoting the development of signs or symptoms in an individual with a *KIT* D816V positive clone, thus increasing the chance of clinical investigation (phenotypic hypothesis). We considered the possibility that clonal somatic changes might affect the analysis, however, we found that SM genomes are relatively simple with only a small proportion of cases showing likely somatic copy number changes or acquired uniparental disomy (Figure S7). Furthermore, apart from isolated cases the genomic regions with somatic changes did not include the risk factors we identified.

Of the 3 significant SNPs identified in this study, the strongest association was seen for rs4616402 at 19q13. Interestingly, this SNP was significantly associated with age of diagnosis in patients with non-advanced disease. This SNP is located in a candidate enhancer and the risk allele is linked to reduced expression of *CEBPA*[60], located 37.3 kb upstream. Another 19q13 SNP, rs78744187, has previously been linked to basophil counts and shown to modulate the activity of a *CEBPA* enhancer[73], however this variant is not in LD with rs4616402 (r^2=0.22). *CEBPA* is an intronless gene which encodes a leucine zipper transcription factor that binds to the CCAAT motif in the promoter of its target genes. It is expressed in myeloid progenitor cells and several studies have defined its critical role in myelopoiesis and malignant transformation of myeloid cells[74]. Of particular relevance, high C/EBPα expression inhibits the production of mast cells from mast/basophil common progenitors whereas low C/EBPα expression inhibits the production of basophils[70]. Although the consequence of reduced *CEBPA* levels in the context of *KIT* D816V remain to be defined, reduced *CEBPA* expression associated with

rs4616402 may be relevant to the fertile ground and phenotypic hypothesis defined above by creating an environment that favors the production of mast cells. It is striking that *CEBPA* or its product C/EBPα is targeted by two other oncogenic tyrosine kinases: BCR-ABL1 downregulates *CEBPA* by a post-transcriptional mechanism[75] and oncogenic FLT3 mutants disrupt C/EBPα function by ERK1/2-mediated phosphorylation[76]. Furthermore, low *CEBPA* expression is commonly seen in acute myeloid leukemia, although the underlying mechanism is unclear[74]. Detailed functional studies are needed to clarify the relationship between *KIT* D816V-driven clonal outgrowth and *CEBPA* expression.

The second most significant SNP, rs4662380, is located at 2q22 within the long non-coding RNA *LINC01412* and associated with higher expression of the nearby gene *TEX41*. Both are of unknown function, but due to the possibility of long range interactions between GWAS signals and target genes it is unclear if either are directly relevant to SM. *ZEB2* is another nearby gene that has been linked to both myeloid and lymphoid leukemias[77; 78] but we found no association between rs4662380 and *ZEB2* expression. Interestingly, rs16823866, a SNP strongly linked to rs4662380, was associated with elevated white blood cells and specifically basophils in three independent population studies[61; 62; 79]. Although the underlying mechanism is unclear, this may be relevant to the phenotypic hypothesis, in that cases with abnormal blood counts may be more likely to be investigated clinically. The final SNP rs13077541 is linked to expression of *TBL1XR1.* This gene has been reported as a fusion partner of *PDGFRB, ROS1*, *RARA* and *RARB* in myeloid malignancies[80-82] but its significance in relation to SM remains to be established.

Supplemental data

Supplemental Data includes 7 figures, 8 tables and additional methods

Declaration of interests

The authors declare no competing interests

Acknowledgements

A full list of the investigators who contributed to the generation of the WTCCC data is available from www.wtccc.org.uk, funding for which was provided by the Wellcome Trust under award 07611. The KORA study was initiated and financed by the Helmholtz Zentrum München—German Research Center for Environmental Health, which is funded by the German Federal Ministry of Education and Research (BMBF) and by the State of Bavaria. Furthermore, KORA research was supported within the

Munich Center of Health Sciences (MC-Health), Ludwig-Maximilians-Universität, as part of LMUinnovativ. The KORA-Study Group consists of A. Peters (speaker), J.Heinrich, R.Holle, R. Leidl, C. Meisinger, K.Strauch and their co-workers, who are responsible for the design and conduct of the KORA studies. We gratefully acknowledge the contribution of all members of field staff conducting the KORA study and we are grateful to all study participants of KORA for their invaluable contributions to this study. The InCHIANTI study baseline (1998-2000) was supported as a "targeted project" (ICS110.1/RF97.71) by the Italian Ministry of Health and in part by the U.S. National Institute on Aging (Contracts: 263 MD 9164 and 263 MD 821336). The Spanish mastocytosis cohort and the Spanish National DNA Bank were supported by grants from the Instituto de Salud Carlos III and FEDER (projects: PI16/00642 and PT17/0015/0044). The Italian cohort of mastocytosis patients was funded by the Associazione Italiana per la Ricerca sul cancro, Mynerva project, 21267. The Novo Nordisk Foundation Center for Basic Metabolic Research is an independent Research Center at the University of Copenhagen partially funded by an unrestricted donation from the Novo Nordisk Foundation (www.metabol.ku.dk). AAZD was supported by a Lady Tata International Award; NCPC, YH, AJC and WJT were supported by Blood Cancer UK grants 13002 and 18007.

Authorship contributions: NCPC and WJT designed and directed the study. GG and WJT performed the data analysis with additional input from AAZD and AJC. ACG-M, TK, JIM-G, MM, PG, IA-T, TH, SB-O, HV, MBM, CB-J, AVM, AO and AR provided samples and/or data from Spanish, Danish, Italian and German patient cohorts. YH prepared samples for genotyping. CG, KS, LF, TT, SB and TMS provided data from control cohorts. GG, NCPC and WJT co-wrote the first draft of the paper and all authors contributed to the final version.

Web resources

OMIM: https://www.omim.org/entry/154800

Wellcome Trust Case Control Consortium: www.wtccc.org.uk

Data availability

Genotyping data is available at ArrayExpress (https://www.ebi.ac.uk/arrayexpress/; accession number E-MTAB-9358). GWAS summary statistics are available at LocusZoom (http://locuszoom.org/).

References

1. Arber, D.A., Orazi, A., Hasserjian, R., Thiele, J., Borowitz, M.J., Le Beau, M.M., Bloomfield, C.D., Cazzola, M., and Vardiman, J.W. (2016). The 2016 revision to the World Health Organization classification of myeloid neoplasms and acute leukemia. Blood 127, 2391-2405.
2. Valent, P., Akin, C., and Metcalfe, D.D. (2017). Mastocytosis: 2016 updated WHO classification and novel emerging treatment concepts. Blood 129, 1420-1427.
3. Cohen, S.S., Skovbo, S., Vestergaard, H., Kristensen, T., Moller, M., Bindslev-Jensen, C., Fryzek, J.P., and Broesby-Olsen, S. (2014). Epidemiology of systemic mastocytosis in Denmark. Br J Haematol 166, 521-528.
4. Arock, M., Sotlar, K., Akin, C., Broesby-Olsen, S., Hoermann, G., Escribano, L., Kristensen, T.K., Kluin-Nelemans, H.C., Hermine, O., Dubreuil, P., et al. (2015). KIT mutation analysis in mast cell neoplasms: recommendations of the European Competence Network on Mastocytosis. Leukemia 29, 1223-1232.
5. Sperr, W.R., Kundi, M., Alvarez-Twose, I., van Anrooij, B., Oude Elberink, J.N.G., Gorska, A., Niedoszytko, M., Gleixner, K.V., Hadzijusufovic, E., Zanotti, R., et al. (2019). International prognostic scoring system for mastocytosis (IPSM): a retrospective cohort study. Lancet Haematol 6, e638-e649.
6. Erben, P., Schwaab, J., Metzgeroth, G., Horny, H.P., Jawhar, M., Sotlar, K., Fabarius, A., Teichmann, M., Schneider, S., Ernst, T., et al. (2014). The KIT D816V expressed allele burden for diagnosis and disease monitoring of systemic mastocytosis. Ann Hematol 93, 81-88.
7. Hoermann, G., Gleixner, K.V., Dinu, G.E., Kundi, M., Greiner, G., Wimazal, F., Hadzijusufovic, E., Mitterbauer, G., Mannhalter, C., Valent, P., et al. (2014). The KIT D816V allele burden predicts survival in patients with mastocytosis and correlates with the WHO type of the disease. Allergy 69, 810-813.
8. Munoz-Gonzalez, J.I., Alvarez-Twose, I., Jara-Acevedo, M., Henriques, A., Vinas, E., Prieto, C., Sanchez-Munoz, L., Caldas, C., Mayado, A., Matito, A., et al. (2019). Frequency and prognostic impact of KIT and other genetic variants in indolent systemic mastocytosis. Blood 134, 456-468.
9. Jawhar, M., Schwaab, J., Alvarez-Twose, I., Shoumariyeh, K., Naumann, N., Lubke, J., Perkins, C., Munoz-Gonzalez, J.I., Meggendorfer, M., Kennedy, V., et al. (2019). MARS: Mutation-Adjusted Risk Score for Advanced Systemic Mastocytosis. J Clin Oncol 37, 2846-2856.
10. Jawhar, M., Schwaab, J., Schnittger, S., Meggendorfer, M., Pfirrmann, M., Sotlar, K., Horny, H.P., Metzgeroth, G., Kluger, S., Naumann, N., et al. (2016). Additional mutations in SRSF2, ASXL1 and/or RUNX1 identify a high-risk group of patients with KIT D816V(+) advanced systemic mastocytosis. Leukemia 30, 136-143.
11. Munoz-Gonzalez, J.I., Jara-Acevedo, M., Alvarez-Twose, I., Merker, J.D., Teodosio, C., Hou, Y., Henriques, A., Roskin, K.M., Sanchez-Munoz, L., Tsai, A.G., et al. (2018). Impact of somatic and germline mutations on the outcome of systemic mastocytosis. Blood Adv 2, 2814-2828.
12. Zhang, L.Y., Smith, M.L., Schultheis, B., Fitzgibbon, J., Lister, T.A., Melo, J.V., Cross, N.C., and Cavenagh, J.D. (2006). A novel K509I mutation of KIT identified in familial mastocytosis-in vitro and in vivo responsiveness to imatinib therapy. Leuk Res 30, 373-378.
13. Wasag, B., Niedoszytko, M., Piskorz, A., Lange, M., Renke, J., Jassem, E., Biernat, W., Debiec-Rychter, M., and Limon, J. (2011). Novel, activating KIT-N822I mutation in familial cutaneous mastocytosis. Exp Hematol 39, 859-865.e852.
14. Zanotti, R., Simioni, L., Garcia-Montero, A.C., Perbellini, O., Bonadonna, P., Caruso, B., Jara-Acevedo, M., Bonifacio, M., and De Matteis, G. (2013). Somatic D816V KIT mutation in a case of adult-onset familial mastocytosis. J Allergy Clin Immunol 131, 605-607.
15. Molderings, G.J., Haenisch, B., Bogdanow, M., Fimmers, R., and Nothen, M.M. (2013). Familial occurrence of systemic mast cell activation disease. PLoS One 8, e76241.

16. Haenisch, B., Nothen, M.M., and Molderings, G.J. (2012). Systemic mast cell activation disease: the role of molecular genetic alterations in pathogenesis, heritability and diagnostics. Immunology 137, 197-205.
17. Daley, T., Metcalfe, D.D., and Akin, C. (2001). Association of the Q576R polymorphism in the interleukin-4 receptor alpha chain with indolent mastocytosis limited to the skin. Blood 98, 880-882.
18. Nedoszytko, B., Niedoszytko, M., Lange, M., van Doormaal, J., Gleń, J., Zabłotna, M., Renke, J., Vales, A., Buljubasic, F., Jassem, E., et al. (2009). Interleukin-13 promoter gene polymorphism -1112C/T is associated with the systemic form of mastocytosis. Allergy 64, 287-294.
19. Rausz, E., Szilágyi, A., Nedoszytko, B., Lange, M., Niedoszytko, M., Lautner-Csorba, O., Falus, A., Aladzsity, I., Kokai, M., Valent, P., et al. (2013). Comparative analysis of IL6 and IL6 receptor gene polymorphisms in mastocytosis. Br J Haematol 160, 216-219.
20. Lange, M., Gleń, J., Zabłotna, M., Nedoszytko, B., Sokołowska-Wojdyło, M., Rębała, K., Ługowska-Umer, H., Niedoszytko, M., Górska, A., Sikorska, M., et al. (2017). Interleukin-31 Polymorphisms and Serum IL-31 Level in Patients with Mastocytosis: Correlation with Clinical Presen-tation and Pruritus. Acta Derm Venereol 97, 47-53.
21. Nedoszytko, B., Lange, M., Renke, J., Niedoszytko, M., Zabłotna, M., Gleń, J., and Nowicki, R. (2018). The Possible Role of Gene Variant Coding Nonfunctional Toll-Like Receptor 2 in the Pathogenesis of Mastocytosis. Int Arch Allergy Immunol 177, 80-86.
22. Nedoszytko, B., Sobalska-Kwapis, M., Strapagiel, D., Lange, M., Górska, A., Elberink, J., van Doormaal, J., Słomka, M., Kalinowski, L., Gruchała-Niedoszytko, M., et al. (2020). Results from a Genome-Wide Association Study (GWAS) in Mastocytosis Reveal New Gene Polymorphisms Associated with WHO Subgroups. Int J Mol Sci 21.
23. Tapper, W., Jones, A.V., Kralovics, R., Harutyunyan, A.S., Zoi, K., Leung, W., Godfrey, A.L., Guglielmelli, P., Callaway, A., Ward, D., et al. (2015). Genetic variation at MECOM, TERT, JAK2 and HBS1L-MYB predisposes to myeloproliferative neoplasms. Nat Commun 6, 6691.
24. Hinds, D.A., Barnholt, K.E., Mesa, R.A., Kiefer, A.K., Do, C.B., Eriksson, N., Mountain, J.L., Francke, U., Tung, J.Y., Nguyen, H.M., et al. (2016). Germ line variants predispose to both JAK2 V617F clonal hematopoiesis and myeloproliferative neoplasms. Blood 128, 1121-1128.
25. (2011). A two-stage meta-analysis identifies several new loci for Parkinson's disease. PLoS Genet 7, e1002142.
26. Wichmann, H.E., Gieger, C., and Illig, T. (2005). KORA-gen--resource for population genetics, controls and a broad spectrum of disease phenotypes. Gesundheitswesen 67 Suppl 1, S26-30.
27. Bosch, X. (2004). Spain to establish national genetic database. Lancet 363, 1044.
28. Julià, A., Domènech, E., Ricart, E., Tortosa, R., García-Sánchez, V., Gisbert, J.P., Nos Mateu, P., Gutiérrez, A., Gomollón, F., Mendoza, J.L., et al. (2013). A genome-wide association study on a southern European population identifies a new Crohn's disease susceptibility locus at RBX1-EP300. Gut 62, 1440-1445.
29. Jorgensen, T., Borch-Johnsen, K., Thomsen, T.F., Ibsen, H., Glumer, C., and Pisinger, C. (2003). A randomized non-pharmacological intervention study for prevention of ischaemic heart disease: baseline results Inter99. Eur J Cardiovasc Prev Rehabil 10, 377-386.
30. Pisinger, C., Vestbo, J., Borch-Johnsen, K., and Jorgensen, T. (2005). Smoking cessation intervention in a large randomised population-based study. The Inter99 study. Prev Med 40, 285-292.
31. Ferrucci, L., Bandinelli, S., Benvenuti, E., Di Iorio, A., Macchi, C., Harris, T.B., and Guralnik, J.M. (2000). Subsystems contributing to the decline in ability to walk: bridging the gap between epidemiology and geriatric practice in the InCHIANTI study. J Am Geriatr Soc 48, 1618-1625.
32. Tanaka, T., Shen, J., Abecasis, G.R., Kisialiou, A., Ordovas, J.M., Guralnik, J.M., Singleton, A., Bandinelli, S., Cherubini, A., Arnett, D., et al. (2009). Genome-wide association study of plasma polyunsaturated fatty acids in the InCHIANTI Study. PLoS Genet 5, e1000338.
33. He, C., Holme, J., and Anthony, J. (2014). SNP genotyping: the KASP assay. Methods Mol Biol 1145, 75-86.

34. (2007). Genome-wide association study of 14,000 cases of seven common diseases and 3,000 shared controls. Nature 447, 661-678.
35. Anderson, C.A., Pettersson, F.H., Clarke, G.M., Cardon, L.R., Morris, A.P., and Zondervan, K.T. (2010). Data quality control in genetic case-control association studies. Nat Protoc 5, 1564-1573.
36. Purcell, S., Neale, B., Todd-Brown, K., Thomas, L., Ferreira, M.A., Bender, D., Maller, J., Sklar, P., de Bakker, P.I., Daly, M.J., et al. (2007). PLINK: a tool set for whole-genome association and population-based linkage analyses. Am J Hum Genet 81, 559-575.
37. Marees, A.T., de Kluiver, H., Stringer, S., Vorspan, F., Curis, E., Marie-Claire, C., and Derks, E.M. (2018). A tutorial on conducting genome-wide association studies: Quality control and statistical analysis. Int J Methods Psychiatr Res 27, e1608.
38. McCarthy, S., Das, S., Kretzschmar, W., Delaneau, O., Wood, A.R., Teumer, A., Kang, H.M., Fuchsberger, C., Danecek, P., Sharp, K., et al. (2016). A reference panel of 64,976 haplotypes for genotype imputation. Nat Genet 48, 1279-1283.
39. Turner, S.D. (2014). qqman: an R package for visualizing GWAS results using Q-Q and manhattan plots. bioRxiv, 005165.
40. Watanabe, K., Taskesen, E., van Bochoven, A., and Posthuma, D. (2017). Functional mapping and annotation of genetic associations with FUMA. Nat Commun 8, 1826.
41. Purcell, S., Cherny, S.S., and Sham, P.C. (2003). Genetic Power Calculator: design of linkage and association genetic mapping studies of complex traits. Bioinformatics 19, 149-150.
42. Coltoff, A., and Mascarenhas, J. (2019). Relevant updates in systemic mastocytosis. Leuk Res 81, 10-18.
43. Stelzer, G., Dalah, I., Stein, T.I., Satanower, Y., Rosen, N., Nativ, N., Oz-Levi, D., Olender, T., Belinky, F., Bahir, I., et al. (2011). In-silico human genomics with GeneCards. Hum Genomics 5, 709-717.
44. Staaf, J., Lindgren, D., Vallon-Christersson, J., Isaksson, A., Goransson, H., Juliusson, G., Rosenquist, R., Hoglund, M., Borg, A., and Ringner, M. (2008). Segmentation-based detection of allelic imbalance and loss-of-heterozygosity in cancer cells using whole genome SNP arrays. Genome Biol 9, R136.
45. Dawoud, A.A.Z., Tapper, W.J., and Cross, N.C.P. (2020). Clonal myelopoiesis in the UK Biobank cohort: ASXL1 mutations are strongly associated with smoking. Leukemia 34, 2660-2672.
46. Ward, L.D., and Kellis, M. (2016). HaploReg v4: systematic mining of putative causal variants, cell types, regulators and target genes for human complex traits and disease. Nucleic Acids Res 44, D877-881.
47. Cooper, G.M., Stone, E.A., Asimenos, G., Green, E.D., Batzoglou, S., and Sidow, A. (2005). Distribution and intensity of constraint in mammalian genomic sequence. Genome Res 15, 901-913.
48. Kircher, M., Witten, D.M., Jain, P., O'Roak, B.J., Cooper, G.M., and Shendure, J. (2014). A general framework for estimating the relative pathogenicity of human genetic variants. Nat Genet 46, 310-315.
49. Boyle, A.P., Hong, E.L., Hariharan, M., Cheng, Y., Schaub, M.A., Kasowski, M., Karczewski, K.J., Park, J., Hitz, B.C., Weng, S., et al. (2012). Annotation of functional variation in personal genomes using RegulomeDB. Genome Res 22, 1790-1797.
50. Buniello, A., MacArthur, J.A.L., Cerezo, M., Harris, L.W., Hayhurst, J., Malangone, C., McMahon, A., Morales, J., Mountjoy, E., Sollis, E., et al. (2019). The NHGRI-EBI GWAS Catalog of published genome-wide association studies, targeted arrays and summary statistics 2019. Nucleic Acids Res 47, D1005-d1012.
51. Ernst, J., and Kellis, M. (2017). Chromatin-state discovery and genome annotation with ChromHMM. Nat Protoc 12, 2478-2492.

52. Hoffman, M.M., Ernst, J., Wilder, S.P., Kundaje, A., Harris, R.S., Libbrecht, M., Giardine, B., Ellenbogen, P.M., Bilmes, J.A., Birney, E., et al. (2013). Integrative annotation of chromatin elements from ENCODE data. Nucleic Acids Res 41, 827-841.
53. Carithers, L.J., and Moore, H.M. (2015). The Genotype-Tissue Expression (GTEx) Project. Biopreserv Biobank 13, 307-308.
54. Zheng, Z., Huang, D., Wang, J., Zhao, K., Zhou, Y., Guo, Z., Zhai, S., Xu, H., Cui, H., Yao, H., et al. (2020). QTLbase: an integrative resource for quantitative trait loci across multiple human molecular phenotypes. Nucleic Acids Res 48, D983-d991.
55. Volders, P.J., Anckaert, J., Verheggen, K., Nuytens, J., Martens, L., Mestdagh, P., and Vandesompele, J. (2019). LNCipedia 5: towards a reference set of human long non-coding RNAs. Nucleic Acids Res 47, D135-d139.
56. Carlevaro-Fita, J., Lanzos, A., Feuerbach, L., Hong, C., Mas-Ponte, D., Pedersen, J.S., and Johnson, R. (2020). Cancer LncRNA Census reveals evidence for deep functional conservation of long noncoding RNAs in tumorigenesis. Commun Biol 3, 56.
57. Pruim, R.J., Welch, R.P., Sanna, S., Teslovich, T.M., Chines, P.S., Gliedt, T.P., Boehnke, M., Abecasis, G.R., and Willer, C.J. (2010). LocusZoom: regional visualization of genome-wide association scan results. Bioinformatics 26, 2336-2337.
58. Võsa, U., Claringbould, A., Westra, H.-J., Bonder, M.J., Deelen, P., Zeng, B., Kirsten, H., Saha, A., Kreuzhuber, R., Kasela, S., et al. (2018). Unraveling the polygenic architecture of complex traits using blood eQTL metaanalysis. bioRxiv, 447367.
59. Westra, H.J., Peters, M.J., Esko, T., Yaghootkar, H., Schurmann, C., Kettunen, J., Christiansen, M.W., Fairfax, B.P., Schramm, K., Powell, J.E., et al. (2013). Systematic identification of trans eQTLs as putative drivers of known disease associations. Nat Genet 45, 1238-1243.
60. Lloyd-Jones, L.R., Holloway, A., McRae, A., Yang, J., Small, K., Zhao, J., Zeng, B., Bakshi, A., Metspalu, A., Dermitzakis, M., et al. (2017). The Genetic Architecture of Gene Expression in Peripheral Blood. Am J Hum Genet 100, 228-237.
61. Kanai, M., Akiyama, M., Takahashi, A., Matoba, N., Momozawa, Y., Ikeda, M., Iwata, N., Ikegawa, S., Hirata, M., Matsuda, K., et al. (2018). Genetic analysis of quantitative traits in the Japanese population links cell types to complex human diseases. Nat Genet 50, 390-400.
62. Astle, W.J., Elding, H., Jiang, T., Allen, D., Ruklisa, D., Mann, A.L., Mead, D., Bouman, H., Riveros-Mckay, F., Kostadima, M.A., et al. (2016). The Allelic Landscape of Human Blood Cell Trait Variation and Links to Common Complex Disease. Cell 167, 1415-1429.e1419.
63. Chen, L., Ge, B., Casale, F.P., Vasquez, L., Kwan, T., Garrido-Martin, D., Watt, S., Yan, Y., Kundu, K., Ecker, S., et al. (2016). Genetic Drivers of Epigenetic and Transcriptional Variation in Human Immune Cells. Cell 167, 1398-1414.e1324.
64. (2012). An integrated encyclopedia of DNA elements in the human genome. Nature 489, 57-74.
65. van Riel, B., and Rosenbauer, F. (2014). Epigenetic control of hematopoiesis: the PU.1 chromatin connection. Biol Chem 395, 1265-1274.
66. Lyons, J.J., Yu, X., Hughes, J.D., Le, Q.T., Jamil, A., Bai, Y., Ho, N., Zhao, M., Liu, Y., O'Connell, M.P., et al. (2016). Elevated basal serum tryptase identifies a multisystem disorder associated with increased TPSAB1 copy number. Nat Genet 48, 1564-1569.
67. Lyons, J.J., Stotz, S.C., Chovanec, J., Liu, Y., Lewis, K.L., Nelson, C., DiMaggio, T., Jones, N., Stone, K.D., Sung, H., et al. (2018). A common haplotype containing functional CACNA1H variants is frequently coinherited with increased TPSAB1 copy number. Genet Med 20, 503-512.
68. Wang, Z., Zhu, B., Zhang, M., Parikh, H., Jia, J., Chung, C.C., Sampson, J.N., Hoskins, J.W., Hutchinson, A., Burdette, L., et al. (2014). Imputation and subset-based association analysis across different cancer types identifies multiple independent risk loci in the TERT-CLPTM1L region on chromosome 5p15.33. Hum Mol Genet 23, 6616-6633.
69. Bao, E.L., Nandakumar, S.K., Liao, X., Bick, A.G., Karjalainen, J., Tabaka, M., Gan, O.I., Havulinna, A.S., Kiiskinen, T.T.J., Lareau, C.A., et al. (2020). Inherited myeloproliferative neoplasm risk affects haematopoietic stem cells. Nature 586, 769-775.

70. Bick, A.G., Weinstock, J.S., Nandakumar, S.K., Fulco, C.P., Bao, E.L., Zekavat, S.M., Szeto, M.D., Liao, X., Leventhal, M.J., Nasser, J., et al. (2020). Inherited causes of clonal haematopoiesis in 97,691 whole genomes. Nature 586, 763-768.
71. Ahmadi, A., Ghaedi, H., Salimian, J., Azimzadeh Jamalkandi, S., and Ghanei, M. (2019). Association between chronic obstructive pulmonary disease and interleukins gene variants: A systematic review and meta-analysis. Cytokine 117, 65-71.
72. Jones, A.V., Chase, A., Silver, R.T., Oscier, D., Zoi, K., Wang, Y.L., Cario, H., Pahl, H.L., Collins, A., Reiter, A., et al. (2009). JAK2 haplotype is a major risk factor for the development of myeloproliferative neoplasms. Nat Genet 41, 446-449.
73. Guo, M.H., Nandakumar, S.K., Ulirsch, J.C., Zekavat, S.M., Buenrostro, J.D., Natarajan, P., Salem, R.M., Chiarle, R., Mitt, M., Kals, M., et al. (2017). Comprehensive population-based genome sequencing provides insight into hematopoietic regulatory mechanisms. Proc Natl Acad Sci U S A 114, E327-e336.
74. Avellino, R., and Delwel, R. (2017). Expression and regulation of C/EBPalpha in normal myelopoiesis and in malignant transformation. Blood 129, 2083-2091.
75. Perrotti, D., Cesi, V., Trotta, R., Guerzoni, C., Santilli, G., Campbell, K., Iervolino, A., Condorelli, F., Gambacorti-Passerini, C., Caligiuri, M.A., et al. (2002). BCR-ABL suppresses C/EBPalpha expression through inhibitory action of hnRNP E2. Nat Genet 30, 48-58.
76. Radomska, H.S., Basseres, D.S., Zheng, R., Zhang, P., Dayaram, T., Yamamoto, Y., Sternberg, D.W., Lokker, N., Giese, N.A., Bohlander, S.K., et al. (2006). Block of C/EBP alpha function by phosphorylation in acute myeloid leukemia with FLT3 activating mutations. J Exp Med 203, 371-381.
77. Bolouri, H., Farrar, J.E., Triche, T., Jr., Ries, R.E., Lim, E.L., Alonzo, T.A., Ma, Y., Moore, R., Mungall, A.J., Marra, M.A., et al. (2018). The molecular landscape of pediatric acute myeloid leukemia reveals recurrent structural alterations and age-specific mutational interactions. Nat Med 24, 103-112.
78. Goossens, S., Wang, J., Tremblay, C.S., De Medts, J., T'Sas, S., Nguyen, T., Saw, J., Haigh, K., Curtis, D.J., Van Vlierberghe, P., et al. (2019). ZEB2 and LMO2 drive immature T-cell lymphoblastic leukemia via distinct oncogenic mechanisms. Haematologica 104, 1608-1616.
79. Vuckovic, D., Bao, E.L., Akbari, P., Lareau, C.A., Mousas, A., Jiang, T., Chen, M.H., Raffield, L.M., Tardaguila, M., Huffman, J.E., et al. (2020). The Polygenic and Monogenic Basis of Blood Traits and Diseases. Cell 182, 1214-1231.e1211.
80. Murakami, N., Okuno, Y., Yoshida, K., Shiraishi, Y., Nagae, G., Suzuki, K., Narita, A., Sakaguchi, H., Kawashima, N., Wang, X., et al. (2018). Integrated molecular profiling of juvenile myelomonocytic leukemia. Blood 131, 1576-1586.
81. Osumi, T., Tsujimoto, S.I., Tamura, M., Uchiyama, M., Nakabayashi, K., Okamura, K., Yoshida, M., Tomizawa, D., Watanabe, A., Takahashi, H., et al. (2018). Recurrent RARB Translocations in Acute Promyelocytic Leukemia Lacking RARA Translocation. Cancer Res 78, 4452-4458.
82. Campregher, P.V., Halley, N.D.S., Vieira, G.A., Fernandes, J.F., Velloso, E., Ali, S., Mughal, T., Miller, V., Mangueira, C.L.P., Odone, V., et al. (2017). Identification of a novel fusion TBL1XR1-PDGFRB in a patient with acute myeloid leukemia harboring the DEK-NUP214 fusion and clinical response to dasatinib. Leuk Lymphoma 58, 2969-2972.
83. Kundaje, A., Meuleman, W., Ernst, J., Bilenky, M., Yen, A., Heravi-Moussavi, A., Kheradpour, P., Zhang, Z., Wang, J., Ziller, M.J., et al. (2015). Integrative analysis of 111 reference human epigenomes. Nature 518, 317-330.

Tables

Table 1. Summary of the most significant SNPs from meta-analysis of stages 1 and 2

SNP	Chr	Location (hg19)	Alleles	RAF	Gene	P_{META}	OR (CI)	I^2
rs4616402	19q13	33,753,555	A/G	0.240	*SLC7A10-CEBPA*	$1.37x10^{-15}$	1.52 (1.37-1.68)	4.2
rs4662380	2q22	145,316,407	C/T	0.189	*LINC01412*	$2.11x10^{-12}$	1.46 (1.32-1.63)	0
rs13077541	3q26	176,925,740	G/A	0.464	*TBL1XR1-LINC00501*	$2.10x10^{-9}$	1.33 (1.21-1.45)	0

SNP, rs identifier from dbSNP; Alleles, risk associated/non-risk associated allele; RAF, risk allele frequency in Europeans from 1000 genomes; P_{META}, fixed effects meta analysis of stages 1 and 2; OR, odds ratio; CI, 95% confidence interval; I^2, heterogeneity index (0-100).

Table 2. Association between the most significant SNPs and clinical phenotypes in the Spanish and Italian cohorts.

		rs4662380		**rs13077541**		**rs4616402**	
Phenotype	**No Cases**	**P value**	**Effect size (CI)**	**P value**	**Effect size (CI)**	**P value**	**Effect size (CI)**
Initial diagnosis (indolent/advanced)	422/26	0.175	0.58 (0.26-1.27)	0.646	0.88 (0.50-1.54)	0.238	0.60 (0.25-1.40)
Sex (F/M)	235/214	0.266	1.18 (0.88 - 1.60)	0.384	1.12 (0.86 - 1.46)	0.904	1.03 (0.65 - 1.61)
Skin lesions (+/-)	275/122	0.638	1.08 (0.77 - 1.51)	0.151	0.81 (0.60 - 1.08)	0.406	1.23 (0.75 - 2.00)
Age at diagnosis	422	0.668	0.55 (-1.97 - 3.07)	0.625	0.67 (-2.02 - 3.35)	0.009	4.41 (1.09 - 7.73)
Tryptase	417	0.452	-0.08 (-0.29 - 0.13)	0.136	-0.17 (-0.39 - 0.05)	0.249	0.17 (-0.12 - 0.45)

Categorical phenotypes: Initial diagnosis (422 indolent vs 26 advanced mastocytosis cases), sex (235 female vs 214 male cases) and skin lesions (275 cases with skin phenotype vs 122 cases without skin phenotype); P value, fixed effects meta analysis of Italian and Spanish Fisher's exact test; effect size, odds ratio; CI, 95% confidence interval**.** Continuous phenotypes: Age at diagnosis and tryptase levels tested in cases with non-advanced phenotype; P value, linear regression; effect size, regression coefficient beta; CI, 95% confidence interval**.**

Figure legends

Figure 1. Genome-wide association of *KIT* D816V-positive mastocytosis

Manhattan plot showing results from the stage-1 meta-analysis of the UK and German cohorts for all 24 chromosomes. Results are plotted for 592,007 SNPs tested as -log10 of the meta-analysis P-values on the y-axis against genomic location on the x-axis. One SNP was identified with genome-wide significance (P-value $<5x10^{-8}$), indicated by the red line, and a further 18 SNPs were identified with suggestive P-values ($<1x10^{-5}$), indicated by the blue line. SNPs selected for replication are highlighted in green, and the three SNPs that reached genome-wide significance after meta-analysis of stages one and two are highlighted in purple.

Figure 2. Forest plots and meta-analysis for three SNPs reaching genome-wide significance.

Forest plots for each SNP associated with SM at a genome-wide level of significance. Odds ratios (OR = ES) and 95% confidence intervals (CI) are displayed on the x-axis. Results are shown for each cohort (UK, German, Spanish, Danish and Italian) and the combined analysis. The SNP subtotals and diamond show the final OR and CI for a fixed effects meta-analysis of all five cohorts and uses I-squared to assess heterogeneity in effect sizes between cohorts.

Figure 3. Regional plots of the imputed stage 1 meta-analysis for SNPs reaching genome-wide significance in the final meta-analysis.

Results from the imputed stage 1 meta-analysis in a region surrounding three SNPs (A rs4616402, B rs4662380 and C rs13077541) which predispose to SM and reached genome-wide significance in the final meta-analysis. In each plot, the leading SNP is indicated by a purple circle and the colour of other SNPs represent the strength of linkage disequilibrium (r^2) with the lead SNP. Protein coding genes and RNA genes are shown in the track below with arrows to indicate the direction of transcription and wider lines representing the location of exons. The lower panel displays the 15 state chromatin track (chromHMM) in primary hematopoietic stem cells (E035) and K562 using data from the NIH Roadmap Epigenomics Consortium[83]. Physical positions are relative to build 37 (hg19) of the human genome.

Figure 1

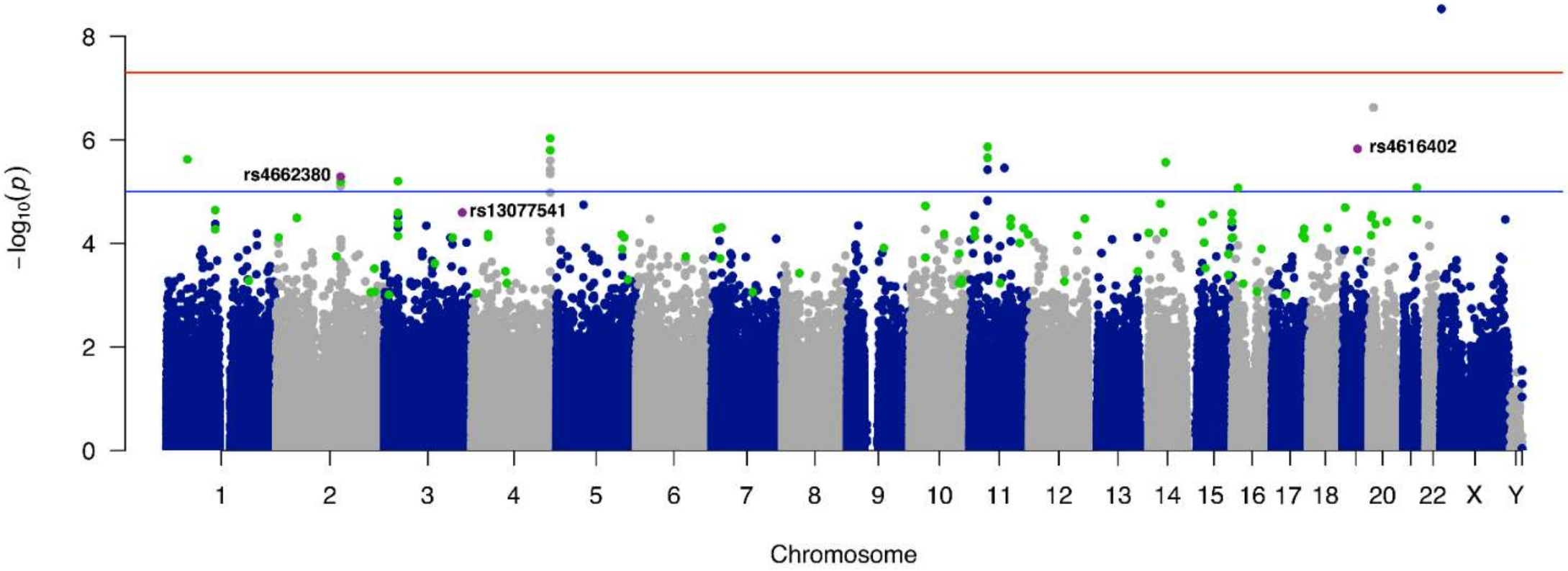
8
6
4
2
0
$-\log_{10}(p)$
rs4662380
rs13077541
rs4616402
1
2
3
4
5
6
7
8
9
10
11
12
13
14
15
16
17
18
20
22
X
Y
Chromosome

Figure 2.

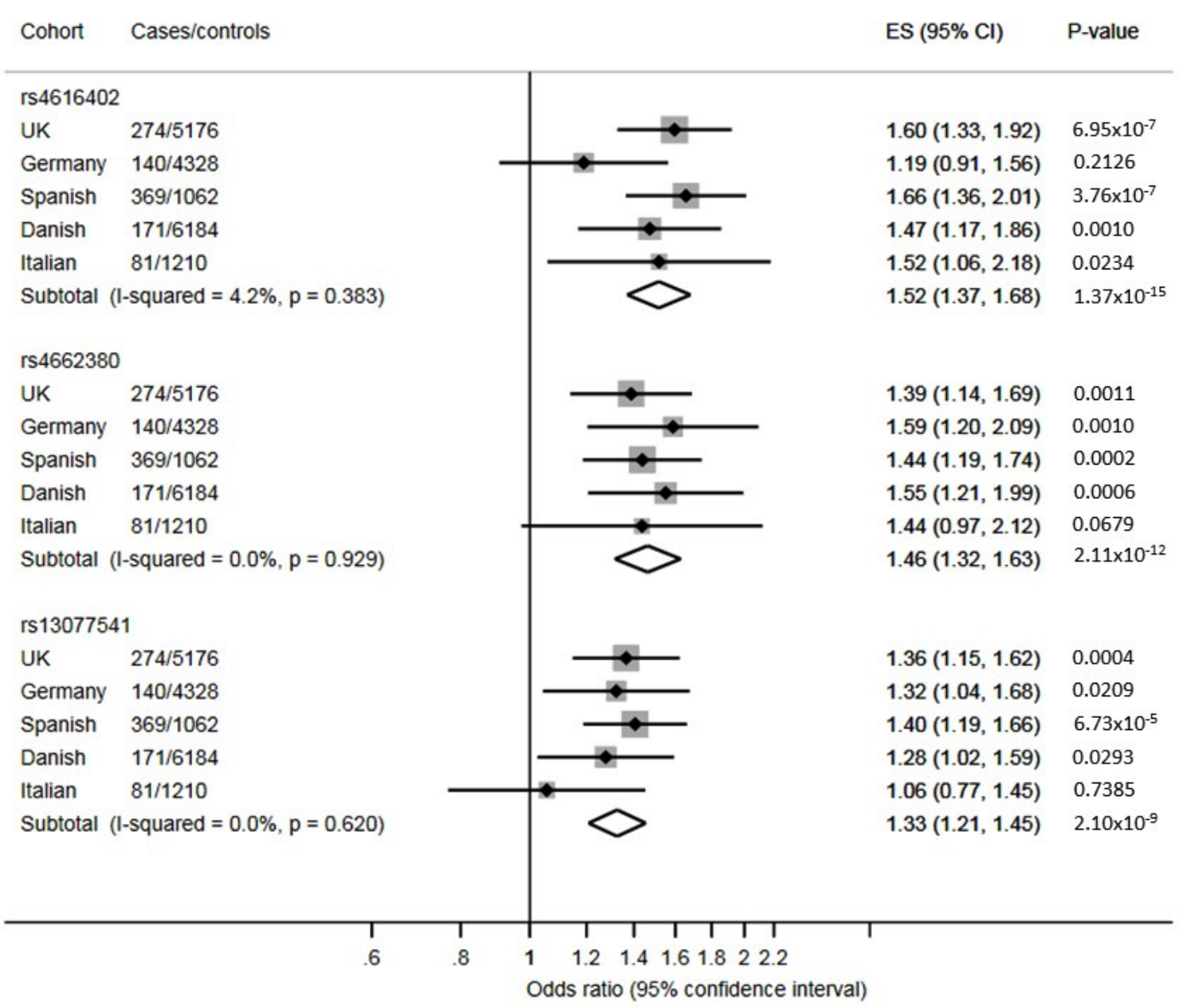
Cohort
Cases/controls
ES (95% CI)
P-value
rs4616402
UK 274/5176 1.60 (1.33, 1.92) 6.95x10-7
Germany 140/4328 1.19 (0.91, 1.56) 0.2126
Spanish 369/1062 1.66 (1.36, 2.01) 3.76x10-7
Danish 171/6184 1.47 (1.17, 1.86) 0.0010
Italian 81/1210 1.52 (1.06, 2.18) 0.0234
Subtotal (I-squared = 4.2%, p = 0.383) 1.52 (1.37, 1.68) 1.37x10-15
rs4662380
UK 274/5176 1.39 (1.14, 1.69) 0.0011
Germany 140/4328 1.59 (1.20, 2.09) 0.0010
Spanish 369/1062 1.44 (1.19, 1.74) 0.0002
Danish 171/6184 1.55 (1.21, 1.99) 0.0006
Italian 81/1210 1.44 (0.97, 2.12) 0.0679
Subtotal (I-squared = 0.0%, p = 0.929) 1.46 (1.32, 1.63) 2.11x10-12
rs13077541
UK 274/5176 1.36 (1.15, 1.62) 0.0004
Germany 140/4328 1.32 (1.04, 1.68) 0.0209
Spanish 369/1062 1.40 (1.19, 1.66) 6.73x10-5
Danish 171/6184 1.28 (1.02, 1.59) 0.0293
Italian 81/1210 1.06 (0.77, 1.45) 0.7385
Subtotal (I-squared = 0.0%, p = 0.620) 1.33 (1.21, 1.45) 2.10x10-9
.6
.8
1
1.2
1.4
1.6
1.8
2
2.2
Odds ratio (95% confidence interval)

Figure 3.

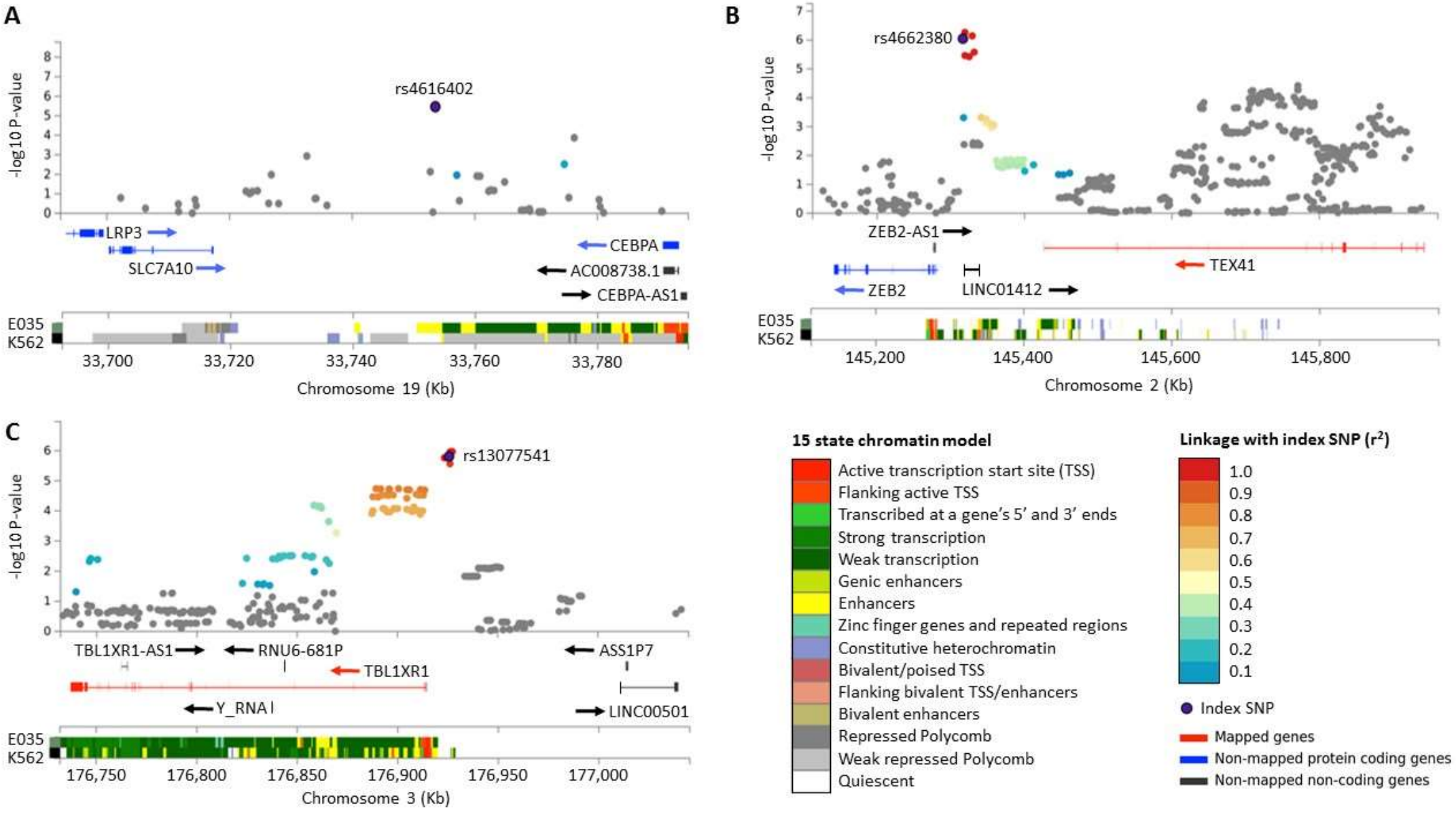
A
rs4616402
-log10 P-value
LRP3
SLC7A10
CEBPA
AC008738.1
CEBPA-AS1
E035
K562
33,700
33,720
33,740
33,760
33,780
Chromosome 19 (Kb)
B
rs4662380
-log10 P-value
ZEB2-AS1
TEX41
ZEB2
LINC01412
E035
K562
145,200
145,400
145,600
145,800
Chromosome 2 (Kb)
C
rs13077541
-log10 P-value
TBL1XR1-AS1
RNU6-681P
ASS1P7
TBL1XR1
Y_RNA
LINC00501
E035
K562
176,750
176,800
176,850
176,900
176,950
177,000
Chromosome 3 (Kb)
15 state chromatin model
Active transcription start site (TSS)
Flanking active TSS
Transcribed at a gene's 5' and 3' ends
Strong transcription
Weak transcription
Genic enhancers
Enhancers
Zinc finger genes and repeated regions
Constitutive heterochromatin
Bivalent/poised TSS
Flanking bivalent TSS/enhancers
Bivalent enhancers
Repressed Polycomb
Weak repressed Polycomb
Quiescent
Linkage with index SNP (r²)
1.0
0.9
0.8
0.7
0.6
0.5
0.4
0.3
0.2
0.1
Index SNP
Mapped genes
Non-mapped protein coding genes
Non-mapped non-coding genes

Genome-wide association study identifies three novel susceptibility loci for *KIT* D816V positive mastocytosis

Gabriella Galatà et al.

Supplementary methods

Discovery and replication cohorts

The primary aim of our study was to identify genetic predisposition to *KIT* D816V positive adult mastocytosis irrespective of disease subtype or clinical phenotype. The stage 1 discovery cohorts were recruited from two diagnostic laboratories (Wessex Regional Genetics Laboratory, UK) and Munich Leukemia Laboratory, Germany) based on (i) referral for investigation of mastocytosis and (ii) testing positive for *KIT* D816V. A breakdown of WHO-defined clinical subtypes and other clinical information was not available for these cases, but <10% were known to have advanced SM. The stage 2 replication cohort was recruited from expert clinical centers in Spain, Denmark and Italy. A breakdown by subtype for stage 2 cases is given in Table S8. Additional diagnostic and clinical variables were only available for the Spanish and Italian cohorts due to ethical limitations regarding consent. The study was approved by UK NRES Committee South West reference 10/H0102/61; Germany: MLL cohort, BLAEK ethics commission, reference 05117; Spain: ethics committee of the University Hospital of Salamanca reference 2016/PI16/00642; Italy: local Ethics Committee, March 12, 2019, protocol number 14560_OSS. The Danish SM study was performed in accordance with the Danish National Committee on Health Ethics.

Additional description of control cohorts

Both WTCC2 and KORA control cohorts comprised two separate studies. In WTCCC2 these were the National Blood Service (NBS, n=2,501) and the British Birth Cohort (BBC, n=2,699) while in KORA these were KORA_A (n=1,938), representing a subset of follow-up F3 of the population based survey KORA S3, and KORA_B (n=2,459), representing an independent subset of KORA S3/F3.

A total of 1,062 healthy controls were recruited from the Spanish National DNA Bank Carlos III (SNDNAB). These individuals were all adults, gave informed consent and were determined to be

healthy based on self-reported health status obtained from personal interviews. See http://www.bancoadn.org for further details.

The InCHIANTI study is a population-based epidemiological study aimed at evaluating the factors that influence mobility in the older population living in the Chianti region in Tuscany, Italy. The details of the study have been previously reported[1]. Briefly, 1616 residents were selected from the population registry of Greve in Chianti (a rural area: 11,709 residents with 19.3% of the population greater than 65 years of age), and Bagno a Ripoli (Antella village near Florence; 4,704 inhabitants, with 20.3% greater than 65 years of age). The participation rate was 90% (n=1453), and the subjects ranged between 21-102 years of age. The study protocol was approved by the Italian National Institute of Research and Care of Aging Institutional Review, the internal Review Board of the National Institute for Environmmental Health Sciences (NIEHS) and by the Medstar Research Institute (Baltimore, MD).

The Inter99 study is a randomized, non-pharmacological intervention study for the prevention of ischemic heart disease[2,3]. In brief, more than 13,000 individuals between 30 and 60 years of age and from 11 municipalities in the south-western part of Copenhagen were randomly selected from the Danish Civil Registration System. Overall, baseline examinations were attended by 6,784 (52%) individuals and genotype information was available for 6,184 individuals. The Inter99 study was approved by the Scientific Ethics Committee of the Capital Region of Denmark (KA98155) and registered as clinical trial (ClinicalTrials.gov; ID-no: NCT00289237). The study protocols were in accordance with the Helsinki declaration and approved by the local ethical committees. The study was performed in accordance with the principles of the Declaration of Helsinki.

Genotyping, imputation and quality control of control cohorts

In brief, SNPs and/or samples were removed from SNDNAB due to low call rate (<98%), HWE (P-value <0.001), heterozygosity (|F|>0,10) or evidence of cryptic relatedness (IBD>0.25). SNPs were then imputed using a two-step process. In the first step, the observed data were phased using SHAPEIT (version 2.r837). In the second step, the phased data were imputed using IMPUTE2 (version 2.3.0) with default settings, an effective population size (-Ne) of 20,000 which is recommended for achieving high accuracy across all population groups and reference haplotypes from phase 3 of the 1,000 Genomes Project[4]. Imputation was performed in 5Mb chunks, as recommended, and then joined. Genotypes with an uncertainty greater than 0.1 were set to missing and the remainder were used as hard calls. SNPs with low imputation quality were excluded (INF0 score <0.6).

Genotyping and QC of the InCHIANTI study has previously been described[5]. In brief, SNPs and/or samples were removed due to low call rate (<97%), HWE (P-value <10^{-4}), heterozygosity (> 0.3), MAF (<1%) and sex mismatches leaving 1,210 samples and 495,343 autosomal SNPs that passed quality control. SNPs were imputed using the Michigan Imputation Server, HRC haplotype reference panel (HRC r1.1 2016) and SNPs with low quality score were removed (INFO ≤0.7).

Genotyping and QC of the Inter99 study has previously been described[6]. Individuals were genotyped using the Illumina HumanOmniExpress-24 SNP arrays (versions v1.0_A and v1.1_A) and the GenomeStudio software. QC filtering was applied before imputation which involved selection of non-monomorphic SNPs, samples with a call rate ≥98%, and SNPs in Hardy–Weinberg equilibrium (p-value > 10^{-5}). Additional SNP genotypes were imputed using Eagle for pre-phasing autosomal SNPs and imputed to the Haplotype Reference Consortia panel (HRC version r1.1) by following the standard protocol on the Michigan imputation server (https://imputationserver.sph.umich.edu/index.html)[7]. All variants included in this study were in Hardy–Weinberg equilibrium ($p > 0.05$) and had high imputation quality scores (INF0≥0.9).

Quality control for mastocytosis cases

At stage-1, QC involved the removal of SNPs and samples with ≥10% missing genotypes, rare SNPs (MAF ≤5%) and duplicate SNPs. Since the cases and controls were genotyped separately, SNPs were excluded if they had modest deviation from Hardy-Weinberg equilibrium (HWE) in controls (P-value <0.001) or extreme deviation in cases (P-value ≤$1x10^{-10}$) which most likely reflects poor genotyping rather than disease association. Samples were also excluded due to outlying autosomal heterozygosity (±3 SD from the mean, Figure S2), if there was a discrepancy between reported and inferred sex based on X chromosome homozygosity or there was evidence for cryptic relatedness based on pairwise measures of identity by state (IBS ≥0.86) for autosomal SNPs in linkage equilibrium (r^2<0.5). Manifest files for each array were used to update strand orientation, genomic location and SNP names. Strand assignments for palindromic SNPs (AT/GC) were checked and corrected if necessary using the Genotype Harmonizer (GH)[8]. The case and control datasets were merged and any non-biallelic SNPs that remained were flipped and removed if unresolved.

A multidimensional scaling analysis (MDS) was used to infer ancestry based on the pairwise measures of IBS. This involved merging the cases and controls with samples from three reference populations from the HapMap consortium (Caucasian, CEU, African, YRI and Asian ASI). The MDS results were inspected by plotting the first (C1) and second (C2) principal components (Figure S3). Samples with

outlying values for C1 (±3 SD from the mean for stage 1 cases and controls and HapMap CEU) were considered ancestry outliers and excluded from further analysis.

The same QC measures were applied to the stage-2 cases with the exceptions that per sample QC measures for heterozygosity, sex-mismatch, cryptic relatedness and non-Caucasian ancestry were not performed due to the small number of SNPs genotyped.

Identification of chromosomal abnormalities

BAF segmentation was run using default settings to exclude SNPs that were non informative (BAF >0.9 or BAF <0.1) or noisy (absolute difference in BAF values between preceding or succeeding SNPs was greater than 0.6). Regions with similar allelic proportions were merged using circular binary segmentation (CBS) and identified as regions of allelic imbalance (AI) if their mean mirrored BAF (mBAF) values were above the default threshold (mBAF≥0.56).

Raw output from BAF segmentation was processed using bedtools[9] to perform further merging of AI regions with a minimum density of 1 SNP per 20 Kb that were separated by less than 5Mb. The merged regions were then scored based on SNP density, heterozygosity rate and coverage. Merged AI regions ≥2Mb in size with confidence scores above an empirically defined threshold (≥9) were selected and compared to the median log2 R ratio (LRR) to determine if they involved copy number gains, losses or were copy number neutral aUPD. The automated calls and genomic locations were confirmed by manual inspection of the BAF plots and revised where necessary to create a final list of mosaic chromosomal abnormalities (mCA) that were plotted alongside a karyotype (Supplementary Figure S6).

Supplementary References

1. Ferrucci L, Bandinelli S, Benvenuti E, et al. Subsystems contributing to the decline in ability to walk: bridging the gap between epidemiology and geriatric practice in the InCHIANTI study. *J Am Geriatr Soc*. 2000;48(12):1618-1625.
2. Husemoen LL, Thomsen TF, Fenger M, Jørgensen HL, Jørgensen T. Contribution of thermolabile methylenetetrahydrofolate reductase variant to total plasma homocysteine levels in healthy men and women. Inter99 (2). *Genet Epidemiol*. 2003;24(4):322-330.
3. Jorgensen T, Borch-Johnsen K, Thomsen TF, Ibsen H, Glumer C, Pisinger C. A randomized non-pharmacological intervention study for prevention of ischaemic heart disease: baseline results Inter99. *Eur J Cardiovasc Prev Rehabil*. 2003;10(5):377-386.
4. Auton A, Brooks LD, Durbin RM, et al. A global reference for human genetic variation. *Nature*. 2015;526(7571):68-74.
5. Tanaka T, Shen J, Abecasis GR, et al. Genome-wide association study of plasma polyunsaturated fatty acids in the InCHIANTI Study. *PLoS Genet*. 2009;5(1):e1000338.

6. Graae AS, Hollensted M, Kloppenborg JT, et al. An adult-based insulin resistance genetic risk score associates with insulin resistance, metabolic traits and altered fat distribution in Danish children and adolescents who are overweight or obese. *Diabetologia*. 2018;61(8):1769-1779.
7. Das S, Forer L, Schonherr S, et al. Next-generation genotype imputation service and methods. *Nat Genet*. 2016;48(10):1284-1287.
8. Deelen P, Bonder MJ, van der Velde KJ, et al. Genotype harmonizer: automatic strand alignment and format conversion for genotype data integration. *BMC Res Notes*. 2014;7:901.
9. Quinlan AR, Hall IM. BEDTools: a flexible suite of utilities for comparing genomic features. *Bioinformatics*. 2010;26(6):841-842.

Supplementary Figures

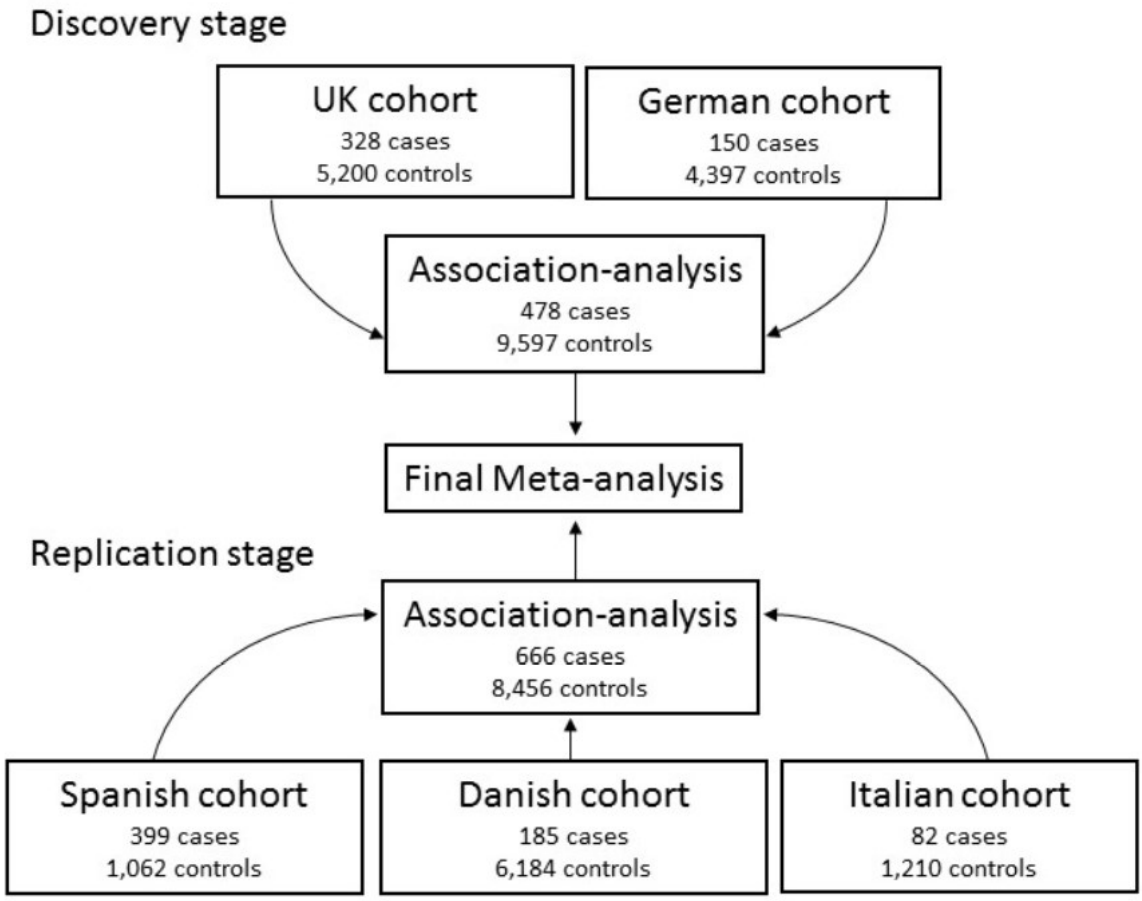

Figure S1. Two stage study design.

An overview of the two stage case control study design and sample numbers, before QC, that were used to investigate inherited predisposition to SM. In the discovery stage, SM patients and healthy controls from the UK and Germany were tested for association using binary logistic regression. Evidence from these separate cohorts was combined using a fixed-effect meta-analysis. SNPs selected for replication were tested in three European cohorts (Spanish, Danish and Italian) using binary logistic regression. Another fixed-effects meta-analysis was used to determine the final effect size and significance levels by combining evidence from the discovery (stage-1) and replication stage (stage-2).

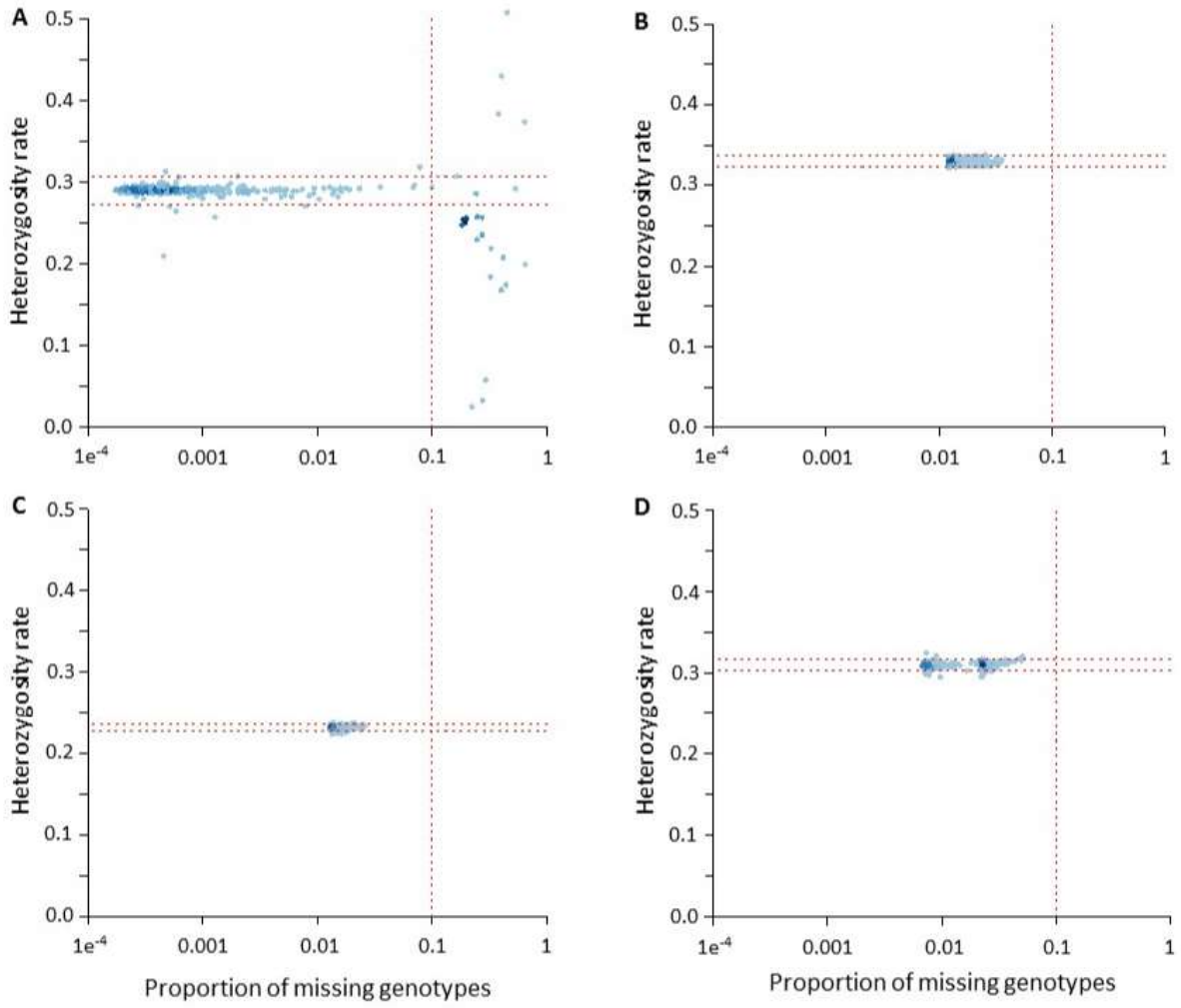

Figure S2. Quality control for autosomal heterozygosity and per sample missingness

A. Stage 1 SM patients from the UK and German cohorts. **B.** Healthy controls from the WTCCC2 cohort. **C.**. Healthy controls from the KORA_A cohort. **D**. Healthy controls from the KORA_B cohort. Horizontal dashed lines indicate the thresholds used to identify samples with outlying levels of heterozygosity in the stage 1 SM patients (±3 SD from the mean). Vertical dashed lines show the threshold used to remove samples with more than 10% missing genotypes.

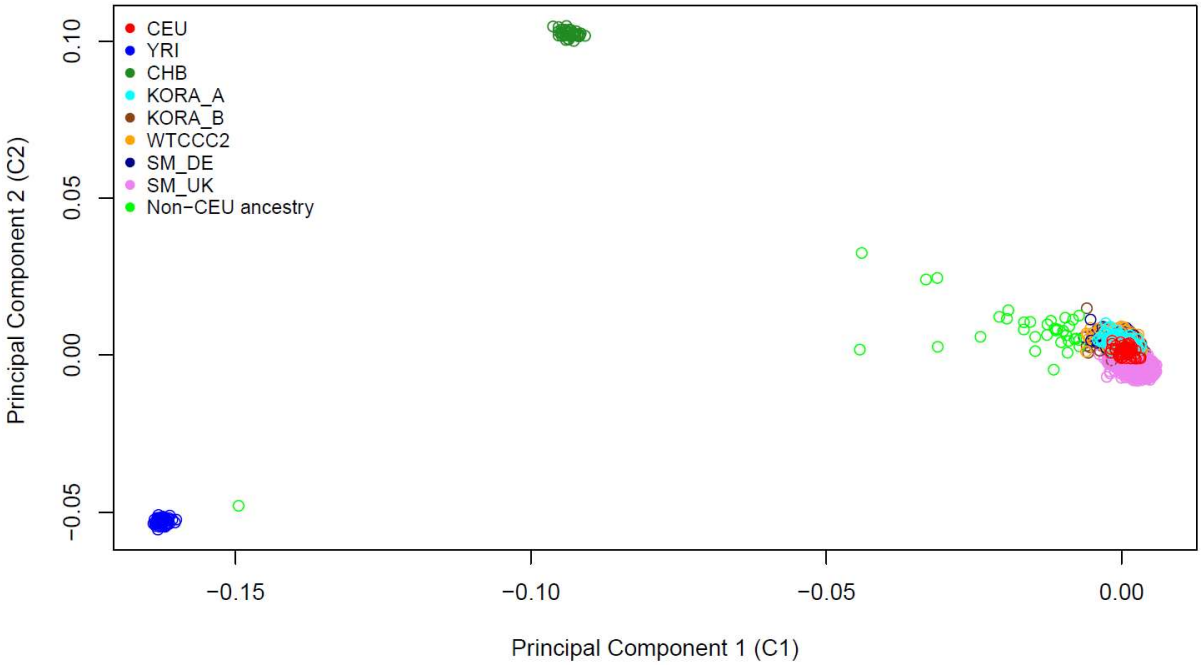

Figure S3. Multidimensional scaling (MDS) plot.

Multidimensional scaling plot generated by plotting the first two components (C1 and C2). SM patients from the UK (purple circles) and Germany (dark blue circles), KORA controls (KORA_A turquoise, KORA_B brown) and WTCCC2 controls (orange), reference populations from HapMap for Utah residents with Northern and Western European ancestry (CEU, red circles), Yoruban individuals from Ibadan, Nigeria (YRI, blue circles), Han Chinese in Beijing, China (dark green circles). Samples with outlying values for C1 (±3 SD from the mean for stage 1 cases and controls and HapMap CEU) were considered ancestry outliers and excluded from further analysis (light green circles).

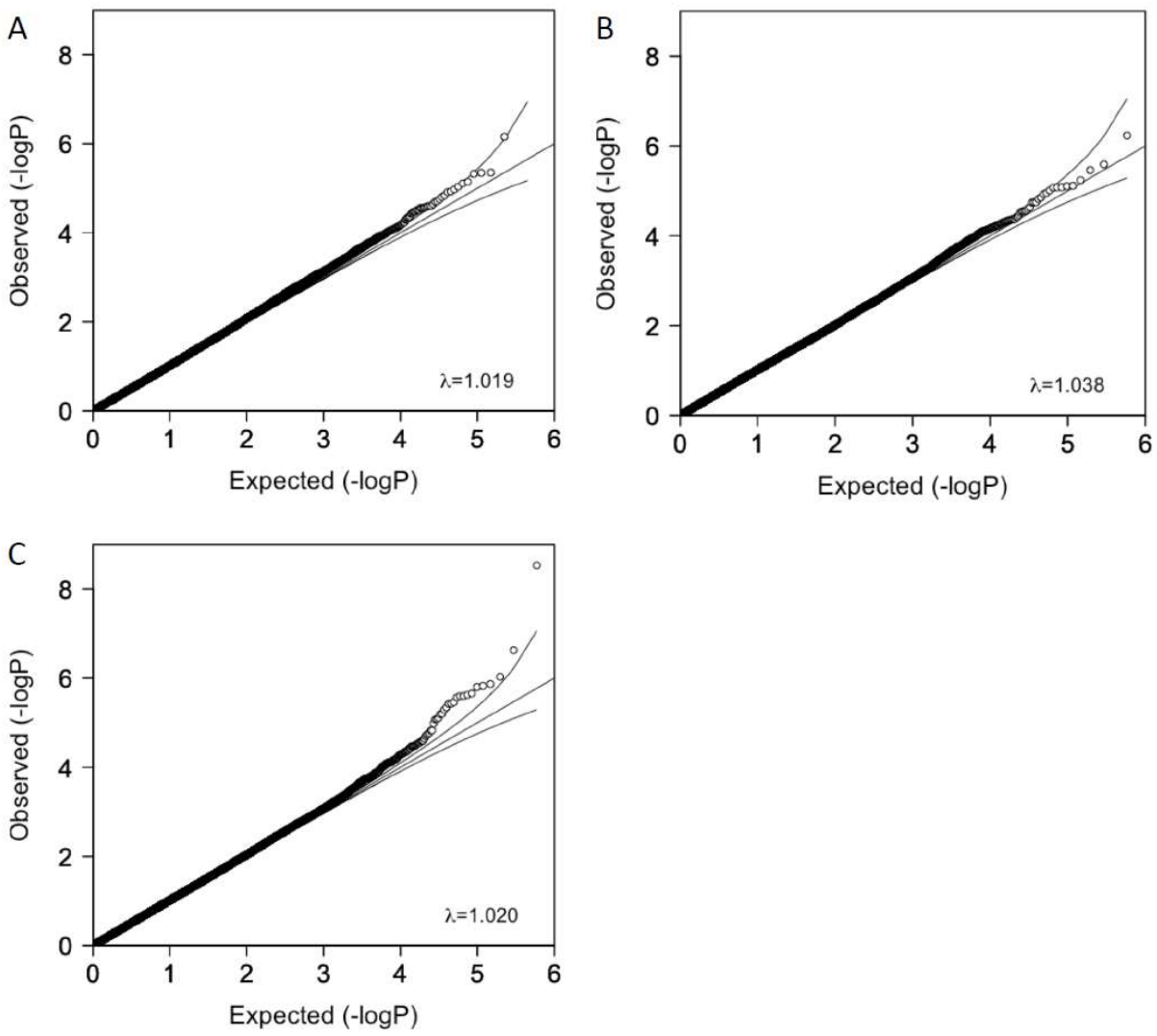

Figure S4. Quantile quantile plots of the stage 1 analyses.

Quantile quantile (QQ)-plots for association with SM at stage-1 for separate analysis of the UK (A) and German (B) cohorts and meta-analysis (C). Expected significance levels under the null hypothesis, where no SNPs are associated with SM, are shown by the straight diagonal lines. The curved lines above and below the diagonal indicate the 95% confidence interval (CI) of the expected P-values. In each plot, the majority of SNPs have observed P-values within the 95% CI until the tail of the distribution where SNPs with P-values less than 10^{-4} start to deviate from the levels of significance that are expected by chance alone.

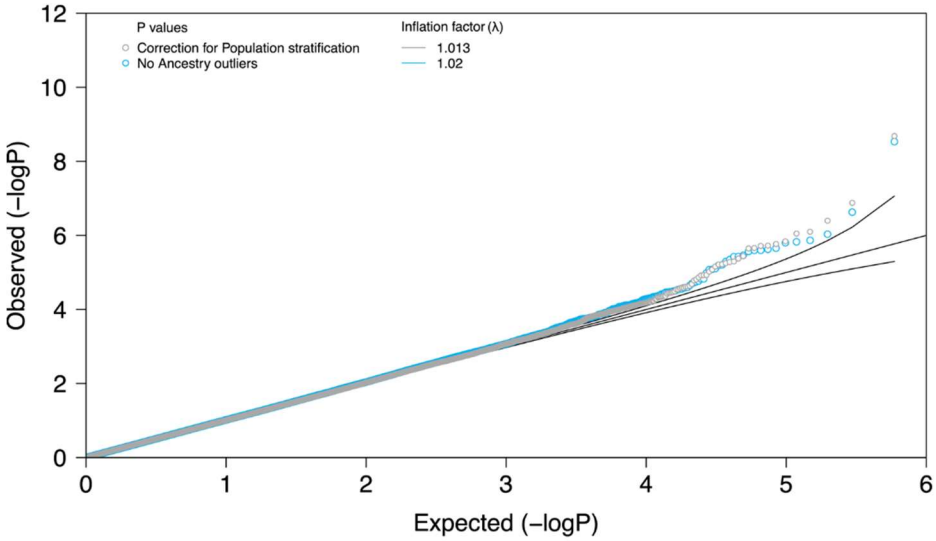

Figure S5. Quantile-quantile plot of the stage 1 meta-analysis with and without correction for population stratification

The analysis without correction excluded 26 ancestry outliers. These samples were included in the analysis which corrected for population stratification using the first two principal components from the MDS analysis.

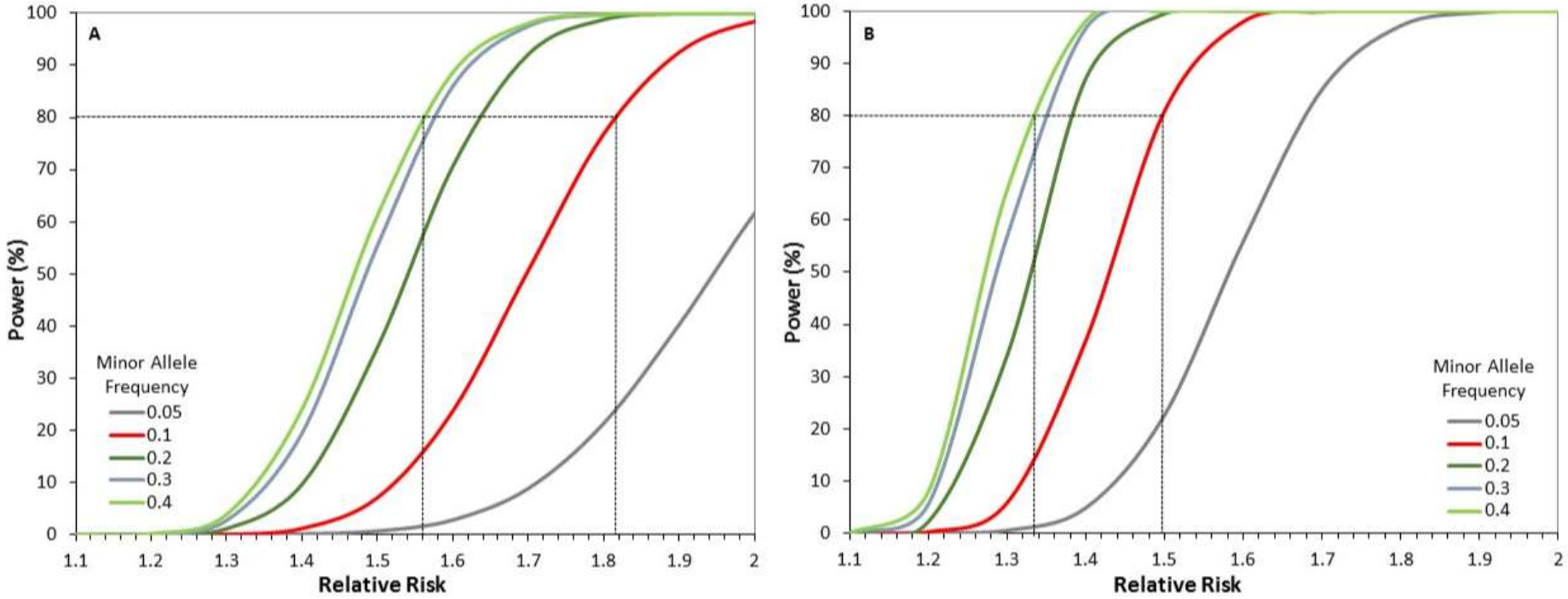

Figure S6. Power to detect SNPs associated with mastocytosis

A. Stage-1 meta-analysis involving 414 cases versus 9,504 healthy controls. B. Meta-analysis of stages 1 and 2 involving 1,060 cases versus 17,960 healthy controls.

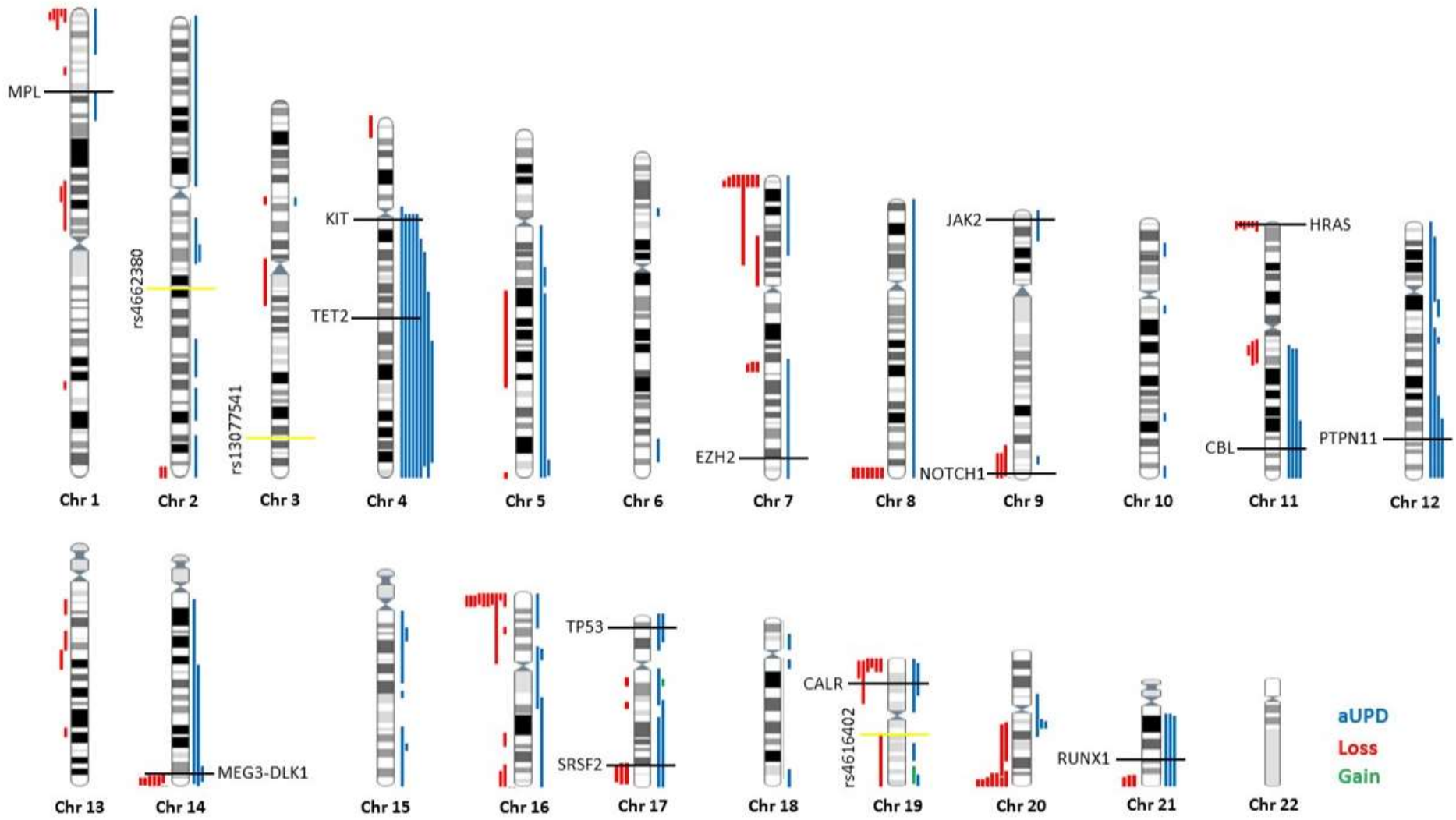

Figure S7. Copy number changes and regions of acquired uniparental disomy in the 414 stage-1 cases